NASA CONTRACTOR REPORT

NASA CR-1645

NASA CR-1645

APPLICATION OF IMPERFECT, REDUCED-STATE RELAY CONTROL TO MODEL-REFERENCE SYSTEMS

by T. M. Taylor

Prepared by
UNIVERSITY OF CONNECTICUT
Storrs, Conn. 06268
for

NATIONAL AERONAUTICS AND SPACE ADMINISTRATION • WASHINGTON, D. C. • AUGUST 1970

1. Report No.	2. Government Accession No.	3. Recipient's Catalog No.
NASA CR-1645		

4. Title and Subtitle	5. Report Date
Application of Imperfect, Reduced-State Relay Control to Model-Reference Systems	August 1970
	6. Performing Organization Code
7. Author(s) T. M. Taylor	8. Performing Organization Report No.
9. Performing Organization Name and Address University of Connecticut School of Engineering Storrs, Conn. 06268	10. Work Unit No. 11. Contract or Grant No. NGL-07-002-002
12. Sponsoring Agency Name and Address National Aeronautics and Space Administration Washington, D. C. 20546	13. Type of Report and Period Covered Contractor Report 14. Sponsoring Agency Code

15. Supplementary Notes

16. Abstract

A new design is proposed for model-reference controllers. In contrast to others, it leads to a controlled system in which the effects of several forms of imperfection may be evaluated. Such forms include relay dead-zone and hysteresis, saturation, additive noise in the switching function or filtered noise, error caused by neglecting transducer dynamics, and error caused by using filtered forms of measured states. The development leads to an estimate of the state bound that could result from these imperfections acting individually or together. Simulation results are obtained for an aircraft roll-control loop.

17. Key Words (Selected by Author(s))	18. Distribution Statement
Calculation of State Bound Filtered Derivatives Model Reference Liapunov Design Reduced State	Unclassified - Unlimited

19. Security Classif. (of this report)	20. Security Classif. (of this page)	21. No. of Pages	22. Price*
U	U	75	$3.00

*For sale by the Clearinghouse for Federal Scientific and Technical Information
Springfield, Virginia 22151

APPLICATION OF IMPERFECT, REDUCED-STATE RELAY CONTROL

TO MODEL-REFERENCE SYSTEMS

Thomas Martin Taylor

The University of Connecticut, Storrs, Connecticut

A new design is proposed for model-reference controllers. In contrast to others, it leads to a controlled system in which the effects of several forms of imperfection may be evaluated. It is shown that the choice of a linear model that has at least one real eigenvalue, facilitates the use of what is termed a natural switching function. Such a switching function is shown to guarantee that the error state vector will monotonically approach the switching plane until it enters a certain planar neighborhood of the switching plane, termed the region of imperfect control. Upon entering this region, the state vector is forced by the natural switching function design to remain in the region for all subsequent time.

Width of the region of imperfect control is shown to be directly proportional to the degree of imperfection. This width is affected additively by all forms of imperfection considered. Such forms include relay dead-zone and hysteresis, saturation, additive noise in the switching function or filtered noise, transducer error and error caused by neglecting transducer dynamics, and error caused by using filtered forms of measured states in place of states that cannot be measured.

The effects of these imperfections on plant-model offset error is evaluated in terms of the reachable set of a linear constant system of order one less than that of plant and model. The input to this system is proportional to the width of the afore-mentioned region of imperfect control. A calculation scheme is developed for the general calculation of such sets.

It is shown that, for purposes of comparing different imperfections, the state bound need not be obtained. Rather, the width of the region of imperfect control may be used. It is demonstrated that this width can be used to evaluate the trade-offs in a reduced-state control

situation. The results support intuition in that a wide band-width filter gives small filter error but accentuates the effects due to noise. Predicted bounds are compared with those that occur in a digital simulation of a model-reference roll-attitude controller. The simulation shows the results to be realistic in the case of a reduced-state controller. In the case of a hysteresis-type imperfection, predicted bounds agree essentially with those that occur.

As an outgrowth of the main development, it is shown that a reduced-state switching function can be shown to yield a practical type of stability for relay control systems. This stability is characterized by a Liapunov function which may decrease in a non-monotone fashion.

Acknowledgements

Research reported herein was performed under National Aeronautics and Space Administration Grant No. NGL-07-002-002 at the University of Connecticut. Computational work was carried out in the University Computer Center under support of this Grant and in part by the National Science Foundation Grant No. GJ-9.

The author is indebted to his associate advisors, Dr. C. H. Knapp and Dr. E. C. Tomastik for their technical suggestions on various aspects of the dissertation. The author is particularly grateful for the encouragement, direction, and technical and editorial suggestions given by his major advisor Dr. D. P. Lindorff. Helpful discussions on certain aspects of the problem with Dr. J. P. LaSalle of Brown University, Dr. K.S. Narendra of Yale University and Dr. R. V. Monopoli of the University of Massachusetts are also gratefully acknowledged.

Thanks are due to the authors students who worked out some of the details for the examples in the third and fifth chapters. Particular mention should be made of the programming assistance of Mr. R. C. DiPetro.

TABLE OF CONTENTS

	Page
CHAPTER I - INTRODUCTION	1
Organization of Thesis	2
A Note to the Reader	3
CHAPTER II - MATHEMATICAL FORMULATIONS	5
System Models	5
Liapunov's Direct Method for Relay Systems	6
Positive Real Test	7
Geometrical Relations of Ellipsoids	9
Monopoli's Bound	10
Conditions for Monotonic Switching Plane Approachment	11
Natural Switching Function	14
Monotonic Decreasing Upper Bound for the Liapunov Function	17
Extreme Projection of the Reachable Set	18
CHAPTER III - RELAY CONTROL SYSTEM: THE CONSTANT CASE	21
Conventional Liapunov Design	22
Augmented System Design	23
Example 3.1	26
Example 3.2	27
CHAPTER IV - THE MODEL-REFERENCE CONTROL PROBLEM	33
Justification of the Relay Model	34
Derivation of Filtered System	38
Natural Switching Function Design	41
Bound on $\|\gamma\|$	44
Design Example	47
Computer Simulation	54
CHAPTER V - DETERMINATION OF BOUND ON STATE VECTOR	59
Reduced-order System	59
Reachable Set Calculation - Second-order Example	60
Reachable Set - General Case	65
CHAPTER VI - CONCLUSIONS	67
BIBLIOGRAPHY	69

LIST OF FIGURES

		Page
2.1	Signum Function of (2.3)	6
2.2	H(s) For a Phase Variable System	8
2.3	Illustrations of (2.15), (2.16) and (2.17)	10
2.4	Illustration of the Regions of (2.22)	12
2.5	Illustration of the Regions of (2.26) for the Case $[\beta_0 \underline{\alpha}^T \underline{c}] > m_1 m_3 / m_2$	13
3.1	Relay Control System	21
3.2	Augmented System	24
3.3	Equivalent Diagram of (3.10)	25
3.4	Implications of Practical Stability on $V(\underline{x})$	27
3.5	Demonstration of (3.23) for (3.18)	28
3.6	The Signum Function and Some Perfect Approximations	29
3.7	The Case Λ Contained in RSPA	30
3.8	The Case Λ Not Contained in RSPA	31
4.1	Model-Reference Controller	33
4.2	Third-Order Model Reference Controller	36
4.3	Equivalent Third-Order Model Reference Controller	37
4.4	Natural Switching Function System	43
4.5	Equivalent Expression of (4.22)	46
4.6	Roll Attitude Control Example	48
4.7	Phase-Variable Representation of Plant and Model	49
4.8	Three Cases of Imperfection Considered	53
4.9	Bounds Estimated for Systems of Figures 4.8a and b	54
4.10	Simulation Results for Cases a and b	55
4.11	Limit Cycle of $\gamma(t)$ for Case c	56
4.12	Comparison of Actual and Estimated Bounds for Case c	58
5.1	Reachable Set of (5.9)	61
5.2	The Filter that Generates y	62
5.3	Calculation of a point p on Reachable Set	63

I. INTRODUCTION

In the early part of the last decade a considerable amount of effort was focused on the general problem of designing controllers for systems exhibiting large parameter uncertainty. This problem was motivated in part by the development of such complex systems in almost all branches of science and it was augmented by the fact that technology of the day demanded tolerances which simply could not be met by extending the classical techniques. Alternative solutions can be summarized in three major categories.

For the case of linear systems, and for some nonlinear systems, the problem was attacked in terms of obtaining a design that was least sensitive to the variable parameters. However, the cost of obtaining a least sensitive design had to be weighed relative to other performance criteria. This led to the optimal formulation which at this time is an unsolved problem inasmuch as it requires measurement of the sensitivity and this is usually not possible.

The fact that, with few exceptions, optimal controllers for linear systems are nonlinear, led many researchers to investigate nonlinear controllers. Most studies focused on particular forms of nonlinearities. This was due in part to the lack of a general nonlinear theory. The learning system was one approach which was not so limited by form. This is a challenging approach to the problem but at this time investigations have not yielded results of any generality.

The third category, which encompasses the work of this dissertation, is identified as adaptive control. There are two general types of adaptation: input adaptation and plant adaptation. The latter involves real-time adjustment of system parameters and although very effective in some cases, no general techniques are available. The former involves adjustment of only the input variable. In particular, attention is directed to a very general design technique attributed to R. W. Bass [13]. The basic idea is to force the input to the time-varying and/or imperfectly specified plant to cause plant states to respond like the respective states of a known linear, time-invariant model, in response to the command input. This scheme is termed model-reference control.

The design proposed by Bass was popularized by L.P. Grayson [1] and further engineered by R. V. Monopoli [2]. A major contribution was made by D. P. Lindorff [3] who modified the design to meet plant saturation constraints. This enhanced the practicality of the technique but two problems remain.

One practical limitation of the technique is that instrumentation of the resulting control requires measurement of all plant states. A related problem is that in order to include transducer dynamics in the design the system order must be augmented, thus requiring the measurement of even more states that most probably cannot be obtained through primary measurements.

Another limitation is that all developments assume an ideal switching element in the generation of the control law. However, no such element exists. In any practical design, one is forced to use an imperfect element which may exhibit deadzone, hysteresis or saturation. A related problem is caused by measurement noise and transducer error.

Organization of Thesis

Chapter II provides the mathematical background for the entire dissertation. This structure provides for continuity of later sections with no loss of rigor.

Chapter III contains some interesting results that pertain to the design of relay controllers but not necessarily to model-reference controllers. It is shown that by means of parallel compensation, a practical type of stability can be guaranteed for a relay control system which does not satisfy the Kalman Positive-Real Test [6]. This enables one to design relay controllers for phase variable linear plants without using highest-order states in the switching function.

The primary results of the dissertation are found in Chapter IV. It is shown that in the case of model-reference controllers the effects of switching function imperfection can be evaluated in a similar fashion. Both contribute to the size of a 'region of imperfect control', the width of which is used in Chapter V to determine a state bound on the tracking error.

The state bound is formulated as the reachable set of a constant linear system. A general means of calculating the boundary of this set is developed in Chapter V and is regarded by the author as one of the major contributions of the thesis. It represents a new method of obtaining the reachable set boundary.

A Note to the Reader

The material in Chapter II could have been included in an appendix. Its importance to the entire development of the thesis merited its inclusion in the main body of the dissertation. The author suggests, however, that the reader omit this chapter in the first reading. It should be used only for referral in sections where a comprehensive understanding is desired.

II Mathematical Formulations

In this section several theorems basic to the thesis are developed. This is done to provide for better continuity of later sections where the train of thought might be obscured by frequent interruptions for theorem statements and proofs.

For the most part, the proofs are informal and consist of demonstrations. In some cases those statements being proved do not deserve the stature of a theorem. For these reasons, and also to avoid a cumbersome structure of theorems and corollaries the statements will be referred to by numbers.

System Models

The first statement is basic to the motivation of the entire thesis investigation for it establishes the relevance of state bounds obtained in Chapter IV to error bounds in equivalent model-reference control systems. In Chapter V the concept is again used to find a system which represents motion of another system confined to a certain region of its state space. It is the following.

> Consider the system $\dot{\underline{y}} = \underline{f}(\underline{y},\underline{p}_y(t),t)$ which has r unknown parameters expressed in the form of vector $\underline{p}_y(t)$ constrained to a region R_y in r space. Consider a second system $\dot{\underline{z}} = \underline{f}(\underline{z},\underline{p}_z(t),t)$ which has r unknown parameters constrained by $\underline{p}_z \in R_z$. Then if $R_z \supset R_y$ it follows that any property that may be implied for all solutions $\underline{z}(t; \underline{z}_0,t_0)$ applies to all solutions $\underline{y}(t; \underline{y}_0,t_0)$ where $\underline{y}_0 = \underline{z}_0$. (2.1)

In essence, this says that the second system is capable of every motion that can be achieved by the first. This results from the fact that since $R_z \supset R_y$ then it is possible to have $\underline{p}_z(t) = \underline{p}_y(t)$ in which case the solutions would be identical. Therefore the set of solutions of the second contains all solutions of the first. Thus any property common to the former applies to the latter. In this sense, the system $\dot{\underline{z}} = \underline{f}(\underline{z},\underline{p}_z(t),t)$ serves as a model for the system $\dot{\underline{y}} = \underline{f}(\underline{y},\underline{p}_y(t),t)$. The model is usually conservative since R_z does not usually equal R_y but this is overshadowed by the fact that one can use (2.1) to obtain properties of the system $\dot{\underline{y}} = \underline{f}(\underline{y}, \underline{p}_y(t),t)$ that could not otherwise be determined.

Liapunov's Direct Method for Relay Systems

The following gives a sufficient condition for asymptotic stability of the origin of the n^{th}-order vector differential equation

$$\dot{\underline{x}} = A\underline{x} - \underline{b}(t)\ \mathrm{Sgn}\ (\underline{\alpha}^T\underline{x}) \tag{2.2}$$

where A is a stability matrix, having all eigenvalues with negative real parts, $\underline{b}(t)$ has all terms bounded.

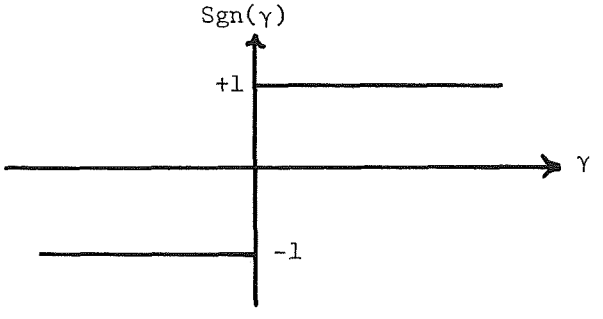

Signum Function of (2.3)
Figure 2.1

The signum function is defined to be

$$\mathrm{Sgn}(\gamma) = \begin{cases} +1 \ ; \ \gamma > 0 \\ 0 \ ; \ \gamma = 0 \\ -1 \ ; \ \gamma < 0 \end{cases} \tag{2.3}$$

as graphed in Figure 2.1. The following is to be proved:

The origin of (2.2) is an asymptotically stable equilibrium point if for some positive definite symmetric nxn matrix Q there exists a matrix P as solution to (2.6)

$$A^T P + P A = -Q \tag{2.4}$$

such that

$$\underline{x}^T P\, \underline{b}(t)\ \mathrm{Sgn}\ (\underline{x}^T\underline{\alpha}) \geq 0. \tag{2.5}$$

for all $\underline{x}$, t.

That the origin $\underline{x} = 0$ is an equilibrium point of (2.2) is easily demonstrated by noting that $\dot{\underline{x}} = \underline{0}$ at $\underline{x} = \underline{0}$. Asymptotic stability is guaranteed by the Second Method of Liapunov [5]. The function

$$V = \underline{x}^T P \underline{x} \tag{2.7}$$

has total time derivative

$$\dot{V} = -\underline{x}^T Q \underline{x} - 2\underline{x}^T P \underline{b}(t) \text{ Sgn } (\underline{\alpha}^T \underline{x}). \tag{2.8}$$

Inasmuch as Q is positive definite (2.5) implies that $\dot{V}$ is negative definite. Furthermore, V is positive definite due to a theorem of Liapunov's that applies to this case where Q is positive definite, A is a stability matrix and P, Q and A are related as in 2.4 [5]. The function V is therefore a Liapunov function for (2.2) thereby guaranteeing asymptotic stability of (2.2)

The sufficient conditions for asymptotic stability given by (2.6) are somewhat cumbersome because of (2.5). However, for the case when $\underline{b}(t)$ can be represented as the product of a time-varying gain $\beta(t)$ and a constant vector $\underline{c}$ where $\beta(t)$ is bounded and positive, that is if

$$\underline{b}(t) = \beta(t)\, \underline{c} \tag{2.9}$$

and $\beta_0 \leq \beta(t) \leq \beta_1$ then (2.5) is satisfied if and only if

$$P\underline{c} = k\underline{\alpha} \tag{2.10}$$

for some positive number k. It should be mentioned that (2.9) is always true of any system that is in phase-variable form and it will be assumed that the resulting $\beta(t)$ is of one sign. The condition (2.10) is useful in searching for a switching function that guarantees asymptotic stability of (2.2). Starting with any positive definite Q and solving (2.4) for P, such a switching function is given by (2.10) to be $\underline{x}^T P \underline{c} = \underline{x}^T \underline{\alpha}$.

Positive Real Test

For analysis purposes (2.6) is practically useless. Given a switching function $\underline{x}^T \underline{\alpha}$, to determine whether it will provide for asymptotic stability of (2.2) by using (2.6) it is necessary to ascertain the existence of a P satisfying (2.10) which is positive definite and which yields through (2.4) a positive definite Q. This involves an extensive search which is usually impractical. However,

for purposes of analysis the following is quite useful. This is a lemma to a theorem of Kalman's [6] presented by Meyer [7]. It pertains to (2.2) with the further condition (2.9), i.e. to

$$\dot{\underline{x}} = A\underline{x} - \beta(t)\ \underline{c}\ \mathrm{Sgn}\ (\underline{\alpha}^T\underline{x}). \tag{2.11}$$

Meyer's lemma is tailored to the particular case of (2.11) where A is a stability matrix. It gives necessary and sufficient conditions on $\underline{\alpha}$ which guarantee the existence of positive definite P and Q and therefore provides equivalent sufficient conditions for asymptotic stability of the origin of (2.11) that are useful for analysis purposes.

The equilibrium state $\underline{x} = 0$ is asymptotically stable if the transfer function

$$H(s) = \underline{\alpha}^T\ [Is-A]^{-1}\ \underline{c} \tag{2.12}$$

satisfies the condition (2.14)

$$\mathrm{Re}[H(s)] \geq 0 \text{ for } \mathrm{Re}\ [s] \geq 0. \tag{2.13}$$

The transfer function H(s) is that relating the nodes u and γ in the signal flow representation of (2.11) found in Figure (2.2). The condition (2.14) will be helpful in eliminating a certain class of switching function candidates.

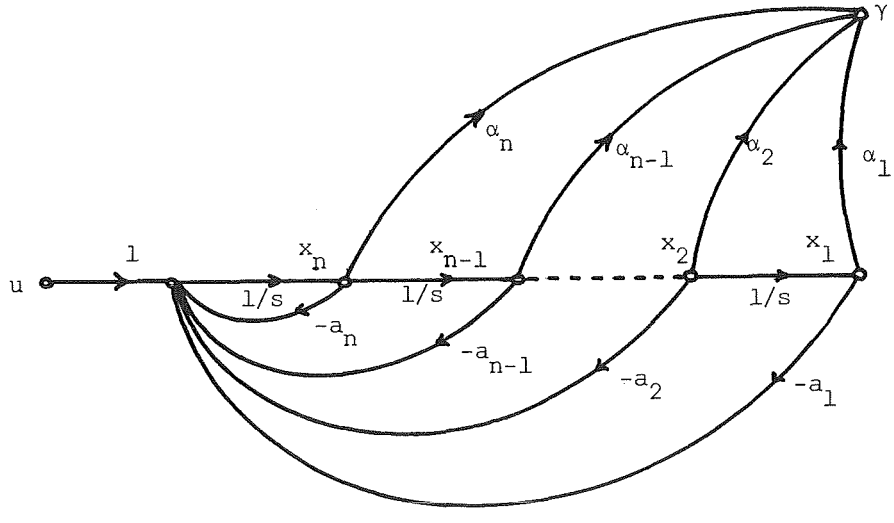

H(s) For a Phase Variable System

Figure 2.2

Geometrical Relations of Ellipsoids

The following geometrical relations are used throughout the thesis. Let the matrices M and N be positive definite.

The smallest value of $\underline{x}^T M \underline{x}$ that occurs on the ellipsoid $\underline{x}^T N \underline{x} = n_0$ is $\frac{1}{\eta_n} n_0$ where η_n is the largest eigenvalue of $M^{-1}N$. (2.15)

The largest value of $\underline{x}^T M \underline{x}$ that occurs on $\underline{x}^T N \underline{x} = n_0$ is $\frac{1}{\eta_1} n_0$ where η_1 is the smallest eigenvalue of $M^{-1}N$. (2.16)

The smallest value of $\underline{x}^T M \underline{x}$ that occurs on the plane $\underline{x}^T \underline{\rho} = n_0$ is $\frac{1}{\eta_n} n_0^2$ where η_n is the largest eigenvalue of $M^{-1}\underline{\rho}\underline{\rho}^T$. (2.17)

These are all proved in the following way. The conditions for an extremum of $\underline{x}^T M \underline{x}$ subject to the constraint $\underline{x}^T N \underline{x} = n_0$ is the following;

$$\frac{\partial}{\partial \underline{x}} [\underline{x}^T M \underline{x} - \frac{1}{\mu} (\underline{x}^T N \underline{x} - n_0)] = \underline{0}. \tag{2.18}$$

This implies that $M\underline{x} = \frac{1}{\mu} N\underline{x}$ rewritten as

$$\mu \underline{x} = M^{-1} N \underline{x} \tag{2.19}$$

implying in turn that μ is an eigenvalue of $M^{-1}N$.
The extreme value is

$$\underline{x}^T M \underline{x} = x^T M \left(\frac{M^{-1} N x}{\mu}\right) = \frac{1}{\mu} n_0. \tag{2.20}$$

Therefore in the case of (2.15) and (2.16) μ must be the largest and smallest eigenvalue of $M^{-1}N$ respectively. The proof for (2.17) follows from symmetry of the quadratic form and noting that planes $\underline{x}^T \underline{\rho} = n_0$ and $\underline{x}^T \underline{\rho} = n_0$ are described by the relation $(\underline{x}^T \underline{\rho})^2 = n_0^2$ or equivalently $\underline{x}^T \rho \rho^T \underline{x} = n_0^2$.

For the case of M and N positive definite, (2.15) determines the largest ellipsoid $\underline{x}^T M \underline{x} = \frac{1}{\eta_n} n_0$ that is completely contained in the ellipsoid $\underline{x}^T N \underline{x} = n_0$. Likewise, (2.16) gives the smallest ellipsoid $\underline{x}^T M \underline{x} = \frac{1}{\eta_1} n_0$ which contains the ellipsoid $\underline{x}^T N \underline{x} = n_0$. The third relation gives the largest ellipsoid $\underline{x}^T M \underline{x} = \frac{1}{\eta_n} n_0^2$ which can be contained between the two planes $\underline{x}^T \underline{\rho} = n_0$ and $\underline{x}^T \underline{\rho} = -n_0$. These relations are illustrated in Figure 2.3 a, b, and c. They will be used in the following which in essence was first proved by Monopoli [2].

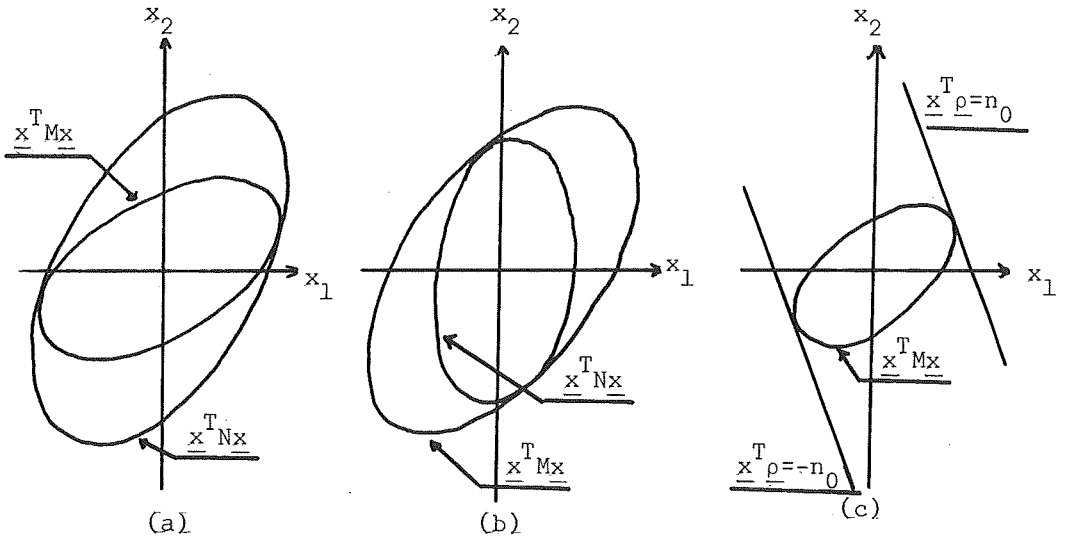

Illustrations of (2.15), (2.16) and (2.17)

Figure 2.3

Monopoli's Bound

Regardless of what switching function is used, solutions of (2.11) will eventually enter and remain in the region (2.22) where

$$\underline{x}^T P \underline{x} \leq \frac{m_1}{m_2} \qquad (2.21)$$

where m_1 is the largest eigenvalue of $[4\beta_1^2 Q^{-1}P \underline{c}\ \underline{c}^T P]$ and m_2 is the smallest eigenvalue of $[P^{-1}Q]$. The term β_1 is the least upper bound of $\beta(t)$.

This is reasonable because $\dot{V}$ for the case of (2.11) is

$$\dot{V} = -\underline{x}^T Q\underline{x} = 2\beta(t)\ \underline{x}^T P\ \underline{c}\ \text{SGN}\ (\underline{\alpha}^T\underline{x}). \tag{2.23}$$

The first term has magnitude which generally increases according to $||\underline{x}||^2$ as evidenced by the relation [11]

$$q_1||\underline{x}||^2 \leq \underline{x}^T Q\underline{x} \leq q_n||x||^2 \tag{2.24}$$

where q_1 and q_n are the smallest and largest eigenvalues of Q respectively. Inasmuch as the second term in (2.23) increases linearly with $||\underline{x}||$ it follows that for $||\underline{x}||$ sufficiently large the gradratic term will dominate.

In the proof the largest value of $\beta(t)$ is used so that the results apply for any value within its range of variation. On any plane $2\beta_1\underline{x}^T P\underline{c} = m_1$ the smallest value of $\underline{x}^T Q\underline{x}$ that occurs is given by (2.17) be be m_1^2/η_n where η_n is the largest eigenvalue of $[4\beta_1^2 Q^{-1}P\underline{c}\ \underline{c}^T P]$ since $P^T = P$. As m_1 increases from zero this resulting smallest value of $\underline{x}^T Q\underline{x}$ increases from zero until at some point it is equal to m_1. That is to say $m_1^2/\eta_n = m_1$, implying that the critical value is $m_1 = \eta_n$. For any larger value of m_1, the corresponding smallest value of $\underline{x}^T Q\underline{x}$ is greater than m_1. Therefore the region where the linear term in (2.23) could dominate the quadratic is limited to the region where $\underline{x}^T Q\underline{x} < m_1$ where $m_1 = \eta_n$. Thus for $\underline{x}^T Q\underline{x} > m_1$ we guarantee $\dot{V} < 0$. The resulting state bound is given in terms of the smallest $V = \underline{x}^T P\underline{x}$ contour that encloses the ellipsoid $\underline{x}^T Q\underline{x} = m_1$. By (2.16)this is $\underline{x}^T P\underline{x} = m_1/m_2$ where m_2 is the smallest eigenvalue of $P^{-1}Q$. The eventual bound is then the region where $\underline{x}^T P\underline{x} \leq m_1/m_2$. Figure 2.4 illustrates the various regions of interest.

Conditions for Monotonic Switching Plane Approachment

The next statement is useful in establishing a bound for solutions of (2.11).

Once the state vector enters the region where $\underline{x}^T P \underline{x} \leq m_1/m_2$ it will for all subsequent time approach the switching plane $\gamma(\underline{x}) = \underline{\alpha}^T \underline{x} = 0$ monotonically provided (2.26)

$$[\beta_0 \underline{\alpha}^T \underline{c}]^2 \geq m_1 m_3 / m_2 \tag{2.25}$$

where m_3 is the largest eigenvalue of $[P^{-1} A^T \underline{\alpha}\underline{\alpha}^T A]$.

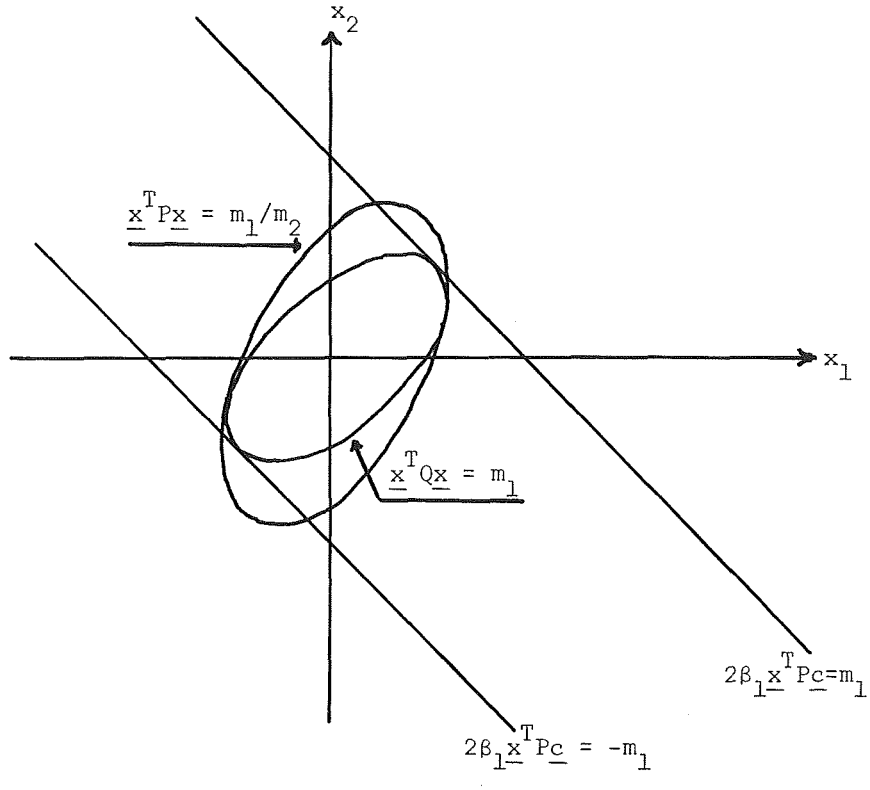

Illustration of the Regions of (2.22)
Figure 2.4

If $\underline{x}$ is approaching the switching plane it must be that the magnitude of γ is decreasing. That is, if $\gamma > 0$ (< 0) it must be that $\dot{\gamma} < 0 (> 0)$. This can be expressed by the condition

$$\text{Sgn}(\dot{\gamma}) = -\text{Sgn}(\gamma) \tag{2.27}$$

where from (2.11)

$$\dot{\gamma} = \underline{\alpha}^T A \underline{x} - \beta(t) \underline{\alpha}^T \underline{c} \ \text{Sgn}(\underline{\alpha}^T \underline{x}). \tag{2.28}$$

The condition (2.27) is satisfied at all points in RSPA, the region of switching plane approachment where

$$|\underline{\alpha}^T A\underline{x}| \leq |\beta_0 \underline{\alpha}^T \underline{x}|. \tag{2.29}$$

An example of such a region is sketched in Figure 2.5.

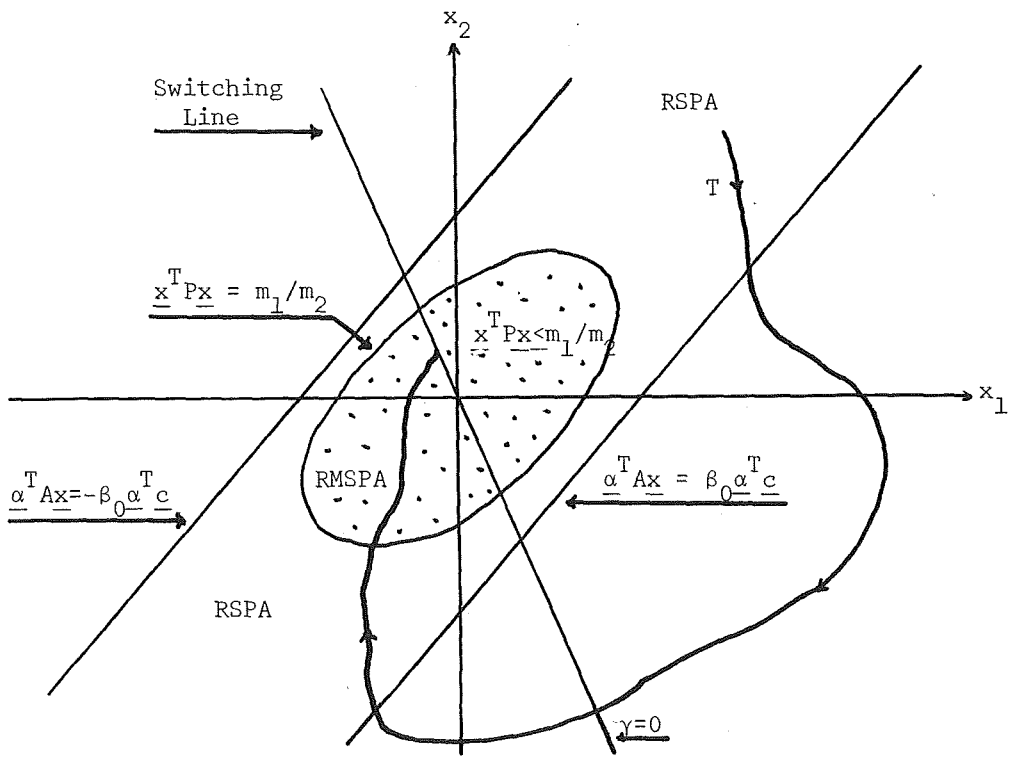

Illustration of the Regions of (2.26) for the Case

$$[\beta_0 \underline{\alpha}^T \underline{c}]^2 > m_1 m_3/m_2$$

Figure 2.5

The trajectory T illustrates that while $\underline{x}$ is in RSPA it is approaching the switching plane, but if it leaves RSPA this need not be true. For monotonic approachment there must be found a subset RMSPA of RSPA which is invariant in the sense that once $\underline{x}$ enters RMSPA it remains for all subsequent time. Such a region would be a region of monotonic switching plane approachment.

The invariant nature of RMSPA, which is where $\underline{x}^T P\underline{x} \leq m_1/m_2$, is guaranteed by (2.22). The condition (2.25) simply guarantees that

$\underline{x}^T P\underline{x} = m_1/m_2$ is entirely contained in RSPA given by (2.29). To show this (2.17) is used to find the minimum value of $\underline{x}^T P\underline{x}$ that occurs on $\underline{\alpha}^T A\underline{x} = \beta_0 \underline{\alpha}^T \underline{c}$, where β_0 is used as a worst case of $\beta(t)$. The minimum value is $\underline{x}^T P\underline{x} = \frac{1}{m_3}[(\beta_0 \underline{\alpha}^T \underline{c})^2]$ which must be greater than m_1/m_2 if RMSPA is to be contained in RSPA. This inequality is expressed in (2.25) and the proof of (2.26) is complete.

Natural Switching Function

In Chapter IV it will be shown to be desirable to have RMSPA equal to RSPA. This necessitates the use of a positive semidefinite Liapunov function. The mathematical basis for such a Liapunov function is provided by LaSalle [8]. Paraphrasing LaSalle's theorem, it is possible to obtain asymptotic stability with the use of a positive semidefinite Liapunov function providing that the function approaches zero monotonically and that motion on the zero manifold is asymptotic to the origin. This will be applied to the system

$$\dot{\underline{x}} = A\underline{x} - \beta(t)\underline{c}\ \mathrm{Sgn}\ (\gamma(\underline{x})) \tag{2.30}$$

where as before A is a stability matrix but furthermore is assumed to have at least one real eigenvalue $-\lambda$ and is assumed to be in phase variable form as follows

$$A = \begin{vmatrix} 0 & 1 & & & \\ & 0 & 1 & & O \\ & & 0 & 1 & \\ & O & & \ddots & \ddots \\ & & & & 1 \\ -a_1 & \cdot & \cdot & \cdot & -a_n \end{vmatrix} \tag{2.31}$$

The input vector is also in phase variable form thus

$$\underline{c} = [0.....1]^T. \tag{2.32}$$

As before we have $0 < \beta_0 \leq \beta(t) \leq \beta_1$. The signum function is defined more generally to be

$$\mathrm{Sgn}\ (\gamma) = \begin{cases} +1 & : \quad \gamma > 0 \\ \sigma & : \quad \gamma = 0; |\sigma| \leq 1. \\ -1 & : \quad \gamma < 0 \end{cases} \tag{2.33}$$

Linear switching is again assumed thus

$$\gamma = \underline{x}^T \underline{\alpha} \tag{2.34}$$

With these assumptions there results the following:

> The origin of (2.30) is asymptotically stable if the switching function coefficient vector $\underline{\alpha}$ is chosen to be the eigenvector of A^T corresponding to the real distinct eigenvalue $-\lambda$ where with no loss in generality we assume $\alpha_n = 1$. (2.35)

To prove this we employ the positive semidefinite function

$$V(\underline{x}) = \frac{1}{2} \gamma^2(\underline{x}). \tag{2.36}$$

This function will decrease monotonically if and only if $|\gamma|$ decreases monotonically. To establish that $|\gamma|$ decreases monotonically consider the derivative

$$\dot{\gamma} = \underline{x}^T A^T \underline{\alpha} - \alpha_n \beta(t) \operatorname{Sgn}(\gamma). \tag{2.37}$$

Since $\underline{\alpha}$ is an eigenvector of A^T with $-\lambda$ corresponding eigenvalue, it results that

$$\underline{x}^T A^T \underline{\alpha} = -\lambda \underline{x}^T \underline{\alpha} = -\lambda\gamma \tag{2.38}$$

and therefore

$$\dot{\gamma} = -\lambda\gamma - \alpha_n \beta(t) \operatorname{Sgn}(\gamma). \tag{2.39}$$

Here $-\lambda$ is a negative number since it is a real eigenvalue of A^T and therefore of A and all eigenvalues of A have negative real part.

The symbol α_n is carried in (2.39) to emphasize the importance of having $\alpha_n > 0$. To show that no generality is lost in setting $\alpha_n = 1$ it is necessary to show that this choice results in all elements of $\underline{\alpha}$ being finite. The n equations represented by

$$A^T \underline{\alpha} = -\lambda \underline{\alpha} \tag{2.40}$$

are

$$\begin{aligned} -a_1 \alpha_n &= -\lambda \alpha_1 \\ \alpha_{i-1} - a_i \alpha_n &= -\lambda \alpha_i; \quad i=2,\ldots n. \end{aligned} \tag{2.41}$$

Assuming $\alpha_n = 1$, leads to the solutions

$$\begin{aligned} \alpha_1 &= a_1 \lambda^{-1} \\ \alpha_i &= \sum_{j=1}^{i} (-1)^{j+1} a_{i-j+1} \lambda^{-j}; \quad i=2,\ldots n. \end{aligned} \tag{2.42}$$

Inasmuch as each a_i is finite and λ is finite it follows that each α_i

is finite.

Returning to the proof, (2.39) is rewritten with $\alpha_n = 1$

$$\dot{\gamma} = -\lambda\gamma - \beta(t)\ \mathrm{Sgn}(\gamma) \tag{2.43}$$

With $\beta(t)$ nonnegative both terms on the right have sign opposite to that of γ. Therefore when γ is positive it is decreasing, and when it is negative it is increasing. This guarantees that γ and consequently $V(\underline{x})$ approach zero monotonically. To guarantee asymptotic stability it only remains to show that motion of (2.30) on the switching plane $\gamma=0$ is asymptotic to the origin.

This can be proved by first noting that motion of the system

$$\dot{\underline{x}} = A\underline{x} \tag{2.44}$$

on the switching plane

$$\gamma = \underline{x}^T\underline{\alpha} = 0 \tag{2.45}$$

is invariant meaning that if a trajectory is initiated on $\gamma=0$ it remains on the switching plane for all subsequent time. Consider any initial condition $\underline{x}_0$ on $\gamma=0$ so that

$$\underline{x}_0^T\ \underline{\alpha} = 0. \tag{2.46}$$

In view of (2.40) and (2.44) it follows that at $\underline{x}_0$

$$\dot{\gamma} = \underline{x}_0^T A^T\ \underline{\alpha} = -\lambda\underline{x}_0^T\ \underline{\alpha} = 0. \tag{2.47}$$

Therefore subsequent motion of (2.44) is confined to the switching plane which must therefore be a manifold of (2.44). Inasmuch as A is a stability matrix (2.44) can only have asymptotically stable manifolds. Motion of (2.30) on $\gamma=0$ is therefore asymptotic to the origin and by LaSalle's theorem (2.30) is asymptotically stable. It should be added that (2.44) is particularly useful because motion of (2.30) on $\gamma=0$ is represented by the following $(n-1)^{st}$-order differential equation

$$\dot{\underline{x}}_r = \begin{vmatrix} 0 & 1 & & \\ & 0 & 1 & \\ & & \ddots & \ddots \\ & & & 1 \\ -\alpha_1 & -\alpha_2 & \cdots & -\alpha_{n-1} \end{vmatrix} \underline{x}_r \tag{2.48}$$

which is the exact same equation that represents motion of (2.44) on

the switching plane $\gamma=0$.

An interesting point arises when in the definition of the signum function (2.33) σ is nonzero. In this case the origin of (2.30) is not an equilibrium state because $\dot{\underline{x}}$ is not identically zero at $\underline{x}=0$ unless $\sigma=0$. This is the reason that the origin of (2.30) has not been termed an equilibrium point. However, (2.35) shows that it has every other property of an asymptotically stable equilibrium point. This is explained by the fact that at $\underline{x}=0$ the signum function with $\sigma\neq 0$ is changing its state from +1 to -1 at an infinite frequency in such a way that its average value over any infinitessimally small interval is zero. But strictly speaking the function is not identically zero. This behavior is due to the idealization of the relay that is employed here; the signum function. The point is that the fact that the origin of (2.30) is not an equilibrium point is of little or no consequence to the physical system.

Monotonic Decreasing Upper Bound for the Liapunov Function

The next theorem applies to the case wherein a positive definite quadratic Liapunov function

$$V = \underline{x}^T P \underline{x} \tag{2.49}$$

having derivative negative definite has been found for an nth-order system. The following implies a condition on a positive definite quadratic function

$$V_r(\underline{x}_r) = \underline{x}_r^T R \, \underline{x}_r \tag{2.50}$$

of a collection $\underline{x}_r$ of the original states.

The function $V_r(\underline{x}_r)$ must satisfy

$$V_r(\underline{x}) \leq \frac{\rho_n}{\eta_1} V(x) \tag{2.51}$$

where ρ_n is the largest eigenvalue of R and η_1 is the smallest eigenvalue of P. (2.52)

Using (2.24) gives

$$\eta_1 \, ||\underline{x}||^2 \leq \underline{x}^T P \underline{x} \tag{2.53}$$

and

$$\underline{x}_r^T R \, \underline{x}_r \leq \rho_n \, ||\underline{x}_r||^2 \tag{2.54}$$

The first implies $||\underline{x}||^2 \leq \frac{1}{\eta_1} \underline{x}^T P \underline{x}$ and the second implies $\underline{x}_r^T R \underline{x}_r \leq \rho_n ||\underline{x}||^2$ since $||\underline{x}_r||^2 \leq ||\underline{x}||^2$. Together this implies

$$\underline{x}_r^T R \underline{x}_r \leq \frac{\rho_n}{\eta_1} \underline{x}^T P \underline{x} \tag{2.55}$$

which is the same as (2.51). This result gives an upper bound on V_r which approaches zero monotonically. This will be used in the next chapter to guarantee a practical type of stability on a reduced-order system.

Extreme Projection of the Reachable Set

The following pertains to a stable constant linear filter having an output e(t) and an input u(t) constrained according to

$$|u(t)| \leq 2L. \tag{2.56}$$

The filter is completely described by its impulse response h(t). It is assumed that e(0) = 0.

The smallest number that $|e|$ cannot exceed in any amount of time is

$$|e|_{lub} = 2L \int_0^\infty |h(\tau)| d\tau \tag{2.57}$$

(2.58)

To prove this it must be shown that (2.57) is the least upper bound on $|e|$. It can be readily shown that this is an upper bound because e(t) is given by

$$e(t) = \int_0^t h(\tau)u(t-\tau)d\tau. \tag{2.58}$$

Thus

$$|e(t)| \leq \int_0^t |h(\tau)| \, |u(t-\tau)| d\tau \tag{2.59}$$

which for any $t \leq \infty$ becomes in light of (2.56)

$$|e| \leq 2L \int_0^\infty |h(\tau)| d\tau \tag{2.60}$$

Therefore $|e|_{lub}$ given by (2.57) is indeed an upper bound. To prove that it is a least upper bound it must be proved that no smaller number

would qualify as a least upper bound. This is shown by the following constructive proof.

Consider the positive nondecreasing sequence $[t_n]=[n]\to\infty$, the sequence of controls $[u_n(t)]$ defined over $0\leq t\leq t_n$ where

$$u_n(t) = 2L \text{ Sgn } [h(t_i-t)] \tag{2.61}$$

and the sequence of resultant outputs

$$\begin{aligned} e_n(t_n) &= 2L \int_0^{t_n} h(\tau) \text{ Sgn } [h(\tau)]d\tau \\ &= 2L \int_0^{t_n} |h(\tau)|d\tau. \end{aligned} \tag{2.62}$$

It follows that as $t_n\to\infty$, $e_n(t_n)\to E$ where

$$E = 2L \int_0^{\infty} |h(\tau)|d\tau. \tag{2.63}$$

Notice that

$$E = |e|_{lub} \tag{2.64}$$

as given by (2.57).

Any smaller candidate, $E-\varepsilon$, for a least upper bound of the filter output must be ruled out since 2.63 guarantees that for some sufficiently large $n(\varepsilon)$, it results that

$$e_n(t_n) > E - \varepsilon. \tag{2.65}$$

Thus (2.57) is proved.

III Relay Control System: The Constant Case

The analysis of relay control systems has posed a serious challenge to the engineer ever since he began to realize the advantages of On-Off control. This challenge was augmented with the later appearance of optimal controllers, some of which were essentially relay controllers. Up to this point, the major effort had been directed at the investigation of conditions for the existence of limit cycles. Only approximate stability conditions were derived by means of inexact techniques such as the Describing Function. The exact analysis was confounded by the fact that even local linearization failed to give in-the-small stability results due to the discontinuous nature of the relay's idealization: the signum function. What was needed was an exact analysis technique for non-linear systems.

This presented itself in the rediscovery and popularization of the Second Method of Liapunov [5] which for the case at hand provides sufficient conditions for asymptotic stability. However, as it will be shown, these conditions require that the relay switching function involve generally all states of the system and necessarily the highest-order-derivative state for the case of phase-variable system. This requirement has limited the practicality of the technique.

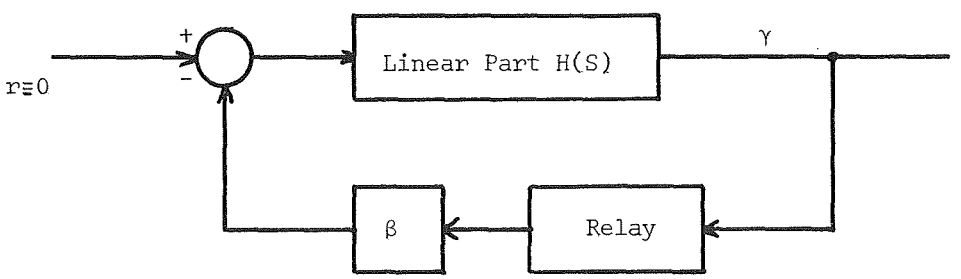

Figure 3.1
Relay Control System

In this chapter, the Liapunov analysis is extended to facilitate the design of relay controllers which do not use highest-derivative state information. The method pertains to the constant parameter case wherein relay feedback is applied to a linear plant having no zeroes. A practical type of stability is guaranteed. The affects of imperfection are evaluated.

Conventional Liapunov Design

The system under investigation is depicted in Figure 3.1. The linear portion is assumed stable and the gain β is a positive number.

An equivalent representation is

$$\dot{\underline{x}} = A\underline{x} - \beta \underline{c}\,\mathrm{Sgn}\gamma \tag{3.1}$$

where A is a constant n x n stability matrix,

$$\gamma = \underline{\alpha}^T \underline{x} = \sum_{i=1}^{n} \alpha_i x_i \tag{3.2}$$

and

$$\underline{c} = [\,0\ 0\ \ldots\ 1\,]^T. \tag{3.3}$$

The signum function is defined as

$$\mathrm{Sgn}\,(\gamma) = \begin{cases} +1 : \gamma > 0 \\ 0 : \gamma = 0 \\ -1 : \gamma < 0 \end{cases} \tag{3.5}$$

and

$$A = \begin{vmatrix} 0 & 1 & & & \\ & 0 & 1 & & \\ & & 0 & 1 & \\ & & & \ddots & \ddots \\ & & & & 0 \quad 1 \\ -a_1 & -a_2 & \ldots & -a_{n-1} & -a_n \end{vmatrix} \tag{3.5}$$

Elements of A are constant and it is assumed that A is a stability matrix. Relating (3.1) to Figure (3.1) it follows that

$$H(s) = \underline{\alpha}^T [Is - A]^{-1} \underline{c}, \tag{3.6}$$

which may be expressed as

$$H(s) = \frac{h_1(s)}{h_2(s)} = \frac{\alpha_n s^{n-1} + \alpha_{n-1} s^{n-2} + \ldots + \alpha_2 s + \alpha_1}{s^n + a_n s^{n-1} + a_{n-1} s^{n-2} + \ldots + a_2 s + a_1} \qquad (3.7)$$

because of the phase-variable structure, Theorem (2.14) gives a sufficient condition for asymptotic stability of the origin of (3.1). It is that

$$\mathrm{Re}[H(s)] \geq 0 \quad \text{for } \mathrm{Re}[s] \geq 0. \qquad (3.8)$$

The point to be made here is that (3.8) can not be satisfied if $\alpha_n = 0$. This can be seen when $|s|$ is large. Let $s = Se^{j\theta}$ and to keep $\mathrm{Re}(s) \geq 0$ we restrict $|\theta| \leq 90°$. $H(s)$ is approximated by α_{n-1}/s^2. Thus, $\mathrm{Re}[H(s)] \simeq \frac{\alpha_{n-1}}{S^2} \mathrm{Cos}2\theta$ which can be negative for the permissable range of θ. This illustrates that the Second Method as applied to the design of the relay control system (3.1) requires that the highest-order state, x_n, must be involved in the switching function. In terms of the analysis of (3.1) this means that the Second Method fails to give stability information when the switching function does not contain x_n. In the next section it will be shown that a design modification will guarantee a practical type of stability.

Augmented System Design

At this point the absence of a sufficient condition that does not require the highest-order state or collection of states for implementation of the switching function forces a design modification which results in a practical type of stability. Sketched in Figure (3.2) the augmented design maintains the same plant-relay configuration but utilizes new states which are generated from the relay output for use in the switching function. If the r^{th}-order filter is represented as

$$F(s) = \frac{f_1(s)}{f_2(s)} = \frac{[\alpha_{n+r} s^{n+r-1} + \alpha_{n+r-1} s^{n+r-2} + \ldots + \alpha_{n+1}]}{[s^{n+r} + a_{n+r} s^{n+r-1} + \ldots + a_{n+1}]} \qquad (3.9)$$

then the following vector equation describes the augmented system

$$\underline{x}' = A'\underline{x}' \; \beta \; \underline{c}' \; \mathrm{Sgn}(\alpha'^{T}\underline{x}') \qquad (3.10)$$

where

$$A' = \left|\begin{array}{c|c} \begin{array}{c} 0\ 1 \\ \ddots \\ 0\ 1 \\ -a_1 \cdots -a_n \end{array} & \bigcirc \\ \hline \bigcirc & \begin{array}{c} 0\ 1 \\ \ddots \\ 0\ 1 \\ -a_{n+1} \cdots -a_{n+r} \end{array} \end{array}\right| \qquad (3.11)$$

$$\underline{\alpha}' = [\alpha_1 \alpha_2 \ldots \alpha_n \ \alpha_{n+1} \ldots \alpha_{n+r}]$$

and (3.12)

$$\underline{c}' = [0\ 0 \ldots . 1 \ \ 0 \ldots . . \ k \ \ ].$$

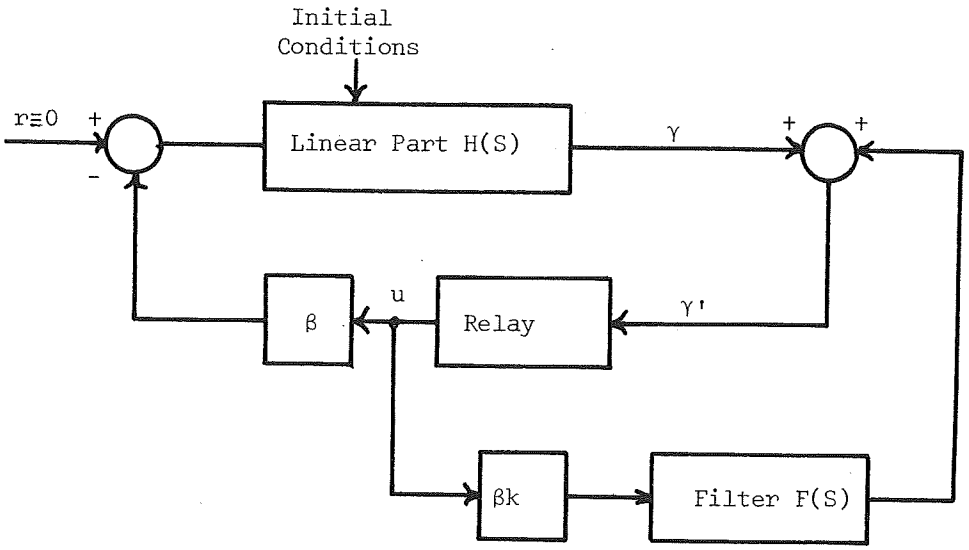

Figure 3.2

Augmented System

For asymptotic stability of (3.10) theorem (2.14) requires that

$$\text{Re } H'(s) \geq 0 \text{ for Re } [s] \geq 0 \qquad (3.13)$$

where in this case

$$H'(s) = \underline{\alpha}'^{T}[Is-A']^{-1}\underline{c}'. \qquad (3.14)$$

From the diagrams of Figure 3.3 which are equivalent to that of Figure 3.2 it becomes apparent that the transfer function H'(s) is simply

$$H'(s) = H(s) + k\,F(s) \tag{3.15}$$

therefore the function

$$H'(s) = [h_1(s)f_2(s) + kf_1(s)h_2(s)]/f_2(s)h_2(s), \tag{3.16}$$

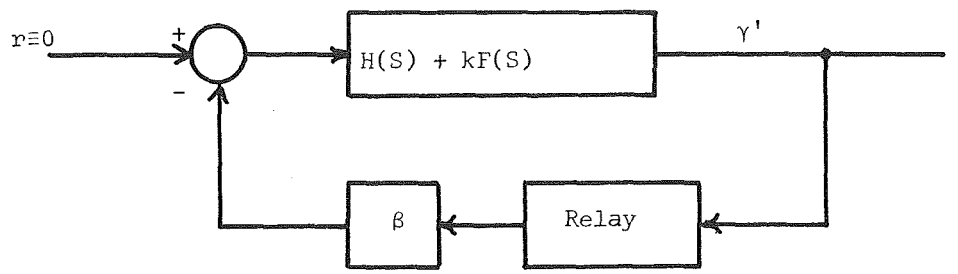

Figure 3.3
Equivalent Diagram of (3.10)

which has a numerator of order one less than the denominator regardless of the term α_n, must satisfy (3.13) for asymptotic stability of (3.10). That is to say, given $h_1(s)$, $h_2(s)$ and β then to achieve asymptotic stability of (3.10) without using the states $\{x_n, x_{n-1}, x_{n-2}, \cdots x_{n-q}\}$ one sets $\alpha_n = \alpha_{n-1} = \alpha_{n-2} = \cdots \alpha_{n-q} = 0$ and seeks coefficients $\alpha_{n-q-1}, \alpha_{n-q-1}, \cdots \alpha_1, \alpha_{n+r}, \alpha_{n+r-1}, \cdots \alpha_{n+1}, a_{n+1}, a_{n+2}, \cdots a_{n+r}$, K and r that make H'(s) satisfy (3.13).

The conditions imposed by (3.13) on H' are not simple to evaluate. Inasmuch as this is a condition for positive realness of H' there are some simplifications that can be made using theorems from the area of network synthesis. This is beyond the scope of this thesis. It suffices to illustrate that for some cases the constants can be found to satisfy the conditions. This is accomplished by the following example.

Example 3.1

The second-order system in the form of

$$\dot{\underline{x}} = \begin{vmatrix} 0 & 1 \\ -1 & -1 \end{vmatrix} \underline{x} - \begin{vmatrix} 0 \\ 1 \end{vmatrix} \mathrm{Sgn}(x_1) \tag{3.17}$$

is to be stabilized with parallel feedback as described above. In this case $H(s) = 1/(s^2+s+1)$ and $\beta = 1$. The filter $F(s)=2/(s+1)$ with $k=-1$ results in $H'(s) = \dfrac{(2s^2 + s + 1)}{(s^3+2s^2+ 2s + 1)}$ which is positive real. Therefore the augmented system

$$\dot{\underline{x}}' = \begin{vmatrix} 0 & 1 & 0 \\ -1 & -1 & 0 \\ 0 & 0 & -1 \end{vmatrix} \underline{x}' - \begin{vmatrix} 0 \\ 1 \\ 1 \end{vmatrix} \mathrm{Sgn}(x_1+2x_3) \tag{3.18}$$

is asymptotically stable. This can be substantiated by means of theorm (2.6) with the choice of positive definite Liapunov function

$$V' = \underline{x}'^{T} \begin{vmatrix} 1 & 1/2 & 0 \\ 1/2 & 2 & -2 \\ 0 & -2 & 3 \end{vmatrix} \underline{x}' \tag{3.19}$$

for which

$$\dot{V}' = -\underline{x}'^{T} \begin{vmatrix} 1 & 3/2 & -2 \\ 3/2 & 3 & -4 \\ -2 & -4 & 6 \end{vmatrix} \underline{x}' - (x_1+2x_3)\ \mathrm{Sgn}(x_1+2x_3) \tag{3.20}$$

which is negative definite. Thus the origin of (3.18) is asymptotically stable.

Having demonstrated the feasibility of the technique it is appropriate to investigate the implications of asymptotic stability of the augmented system (3.10) on the original system (3.1).

It should be observed that the existence of a Liapunov function

$$V'(\underline{x}') = \underline{x}'^{T} P'\underline{x}' \tag{3.21}$$

for the system (3.10),does not guarantee that the function

$$V(\underline{x}) = \underline{x}^{T}P\underline{x}, \tag{3.22}$$

is a Liapunov function for the system (3.1) where P is derived from P'

by the relation $p_{ij}=p_{ij}$; $i,j \leq n$. That is to say, the fact that the positive definite function V' has derivative negative definite does not imply that the positive definite function V has derivative negative definite. One important property that is implied is that

$$V(\underline{x}) \leq \frac{\rho_n}{\eta_1} V'(\underline{x}) \tag{3.23}$$

where ρ_n is the largest eigenvalue of P and η_1 is the smallest eigenvalue of P'. This is an application of theorem (2.52). As illustrated in Figure 3.4. (3.23) implies that $V(\underline{x})$ is bounded

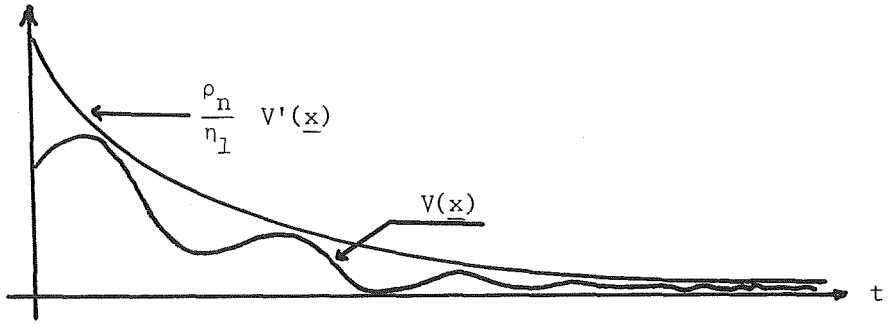

Figure 3.4
Implications of Practical Stability on $V(\underline{x})$

above by a monotonic decreasing function which approaches zero in the limit as time gets large. This implies that $V(\underline{x})$ approaches zero but allows for this to happen oscillatingly. This guarantees a practical type of stability for (3.1) because it implies that $||x|| \to 0$ as $t \to \infty$. This is further illustrated by the following example.

Example 3.2

Continuing with Example 3.1 we have

$$P' = \begin{vmatrix} 1 & 1/2 & 0 \\ 1/2 & 2 & -2 \\ 0 & -2 & 3 \end{vmatrix} \quad \text{and} \quad P = \begin{vmatrix} 1 & 1/2 \\ 1/2 & 2 \end{vmatrix}$$

for which $\eta_1(P') = 0.284$ and $\rho_n(P) = .793$. The system (3.18) was simulated by computer with initial condition $\underline{x}' = [5 \;\; 5 \;\; 2.5]^T$. In

Figure (3.5) $\frac{\rho_n}{\eta_1} V'(\underline{x}')$ which is (2.8) $\underline{x}'^T P' \underline{x}'$ is plotted along with $V(\underline{x})$ given by $\underline{x}^T P \underline{x}$. The results bear out (3.23)

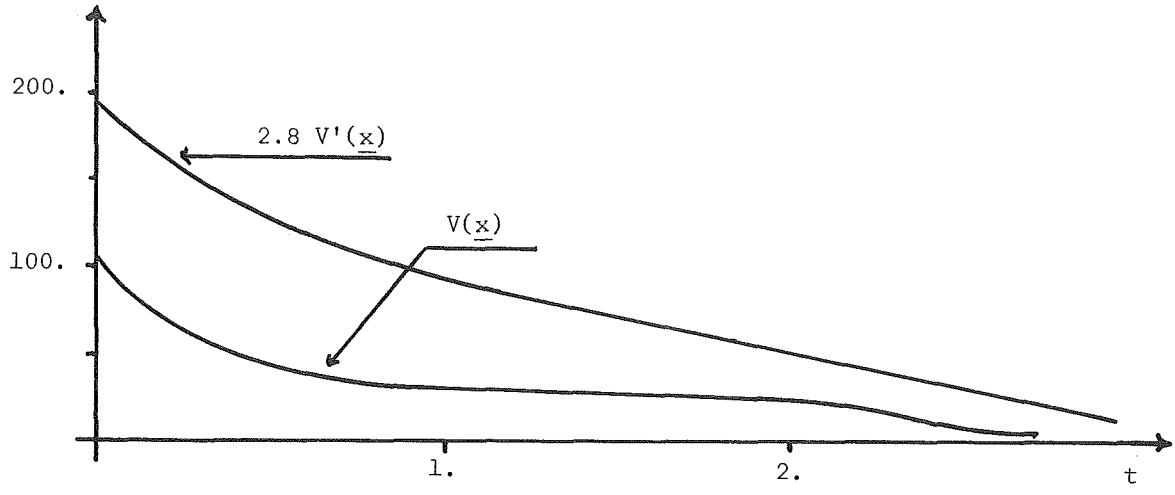

Figure 3.5
Demonstration of (3.23) for (3.18)

To complete this discussion of the augmented system design the sensitivity to imperfection should be evaluated. Imperfection can result in practice from the use of a non-ideal relay that may better be characterized by a deadzone element, a hysteresis element, or possibly a saturating linear element, all of which are sketched in Figure (3.6). It may also occur due to transducer error or measurement noise bound in magnitude by some number L. Common to all such imperfections is the fact that if the magnitude of the switching function γ is greater that L the imperfection has no effect. That is to say, in the case of the imperfect elements of Figure 3.6, the outputs are identical to that of the Signum function if $|\gamma| \geq L$ and in the case of transducer error or measurement noise bounded in magnitude by L, the sign of the sum $\gamma \pm L$ is the same as that of γ. For this reason, the affects of imperfection are only of consequence in the state space region Ω' given by

$$\Omega' = [\underline{x}' : |\gamma'(\underline{x}')| \leq L] \tag{3.24}$$

where

$$\gamma' = \underline{\alpha}'^{T}\underline{x}' \tag{3.25}$$

This is termed the 'region of imperfect control'. It consists of the region between the hyperplanes $\gamma'=L$ and $\gamma'= -L$ which are parallel to and equidistant from the switching plane $\gamma' = 0$.

In this thesis the affects of imperfection are evaluated in terms of an estimate of the state bound that would result. Calculation of this bound is treated in Chapter V. That discussion relies

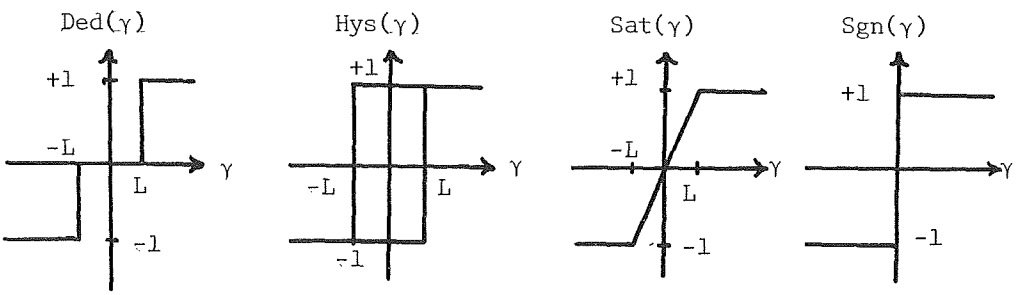

Figure 3.6

The Signum Function and Some Imperfect Approximations

on the property that the state vector $\underline{x}'$ will eventually enter Ω' and remain there for all subsequent time. This must be the case even in the presence of imperfection.

Theorem (2.22) gives a result which is useful here because it applies to the augmented system even with unlimited imperfection, that is, unbounded L. In this case (2.22) implies that for any amount of imperfection, solutions of (3.10) will eventually enter the region Λ defined by

$$\Lambda=\{\underline{x}' ; x'^{T}P'\underline{x}' \leq M_1/M_2\} \tag{3.26}$$

where M_1 is the largest eigenvalue of $[4\beta^2 Q'^{-1} P' C' C'^T P']$, M_2 is the smallest eigenvalue of $[P'^{-1} Q']$ and $Q' = -[A'^T P' + P'A']$.

A critical point is dependent on whether or not Λ is contained in the region of switching plane approachment (RSPA) given according to (2.29) for (3.10) as

$$\text{RSPA} = \{\underline{x}' : |\alpha'^T A' \underline{x}'| \leq \beta \, \underline{\alpha}^T \underline{c} \}. \tag{3.27}$$

If Λ is contained in RSPA as sketched in Figure 3.7 then once a

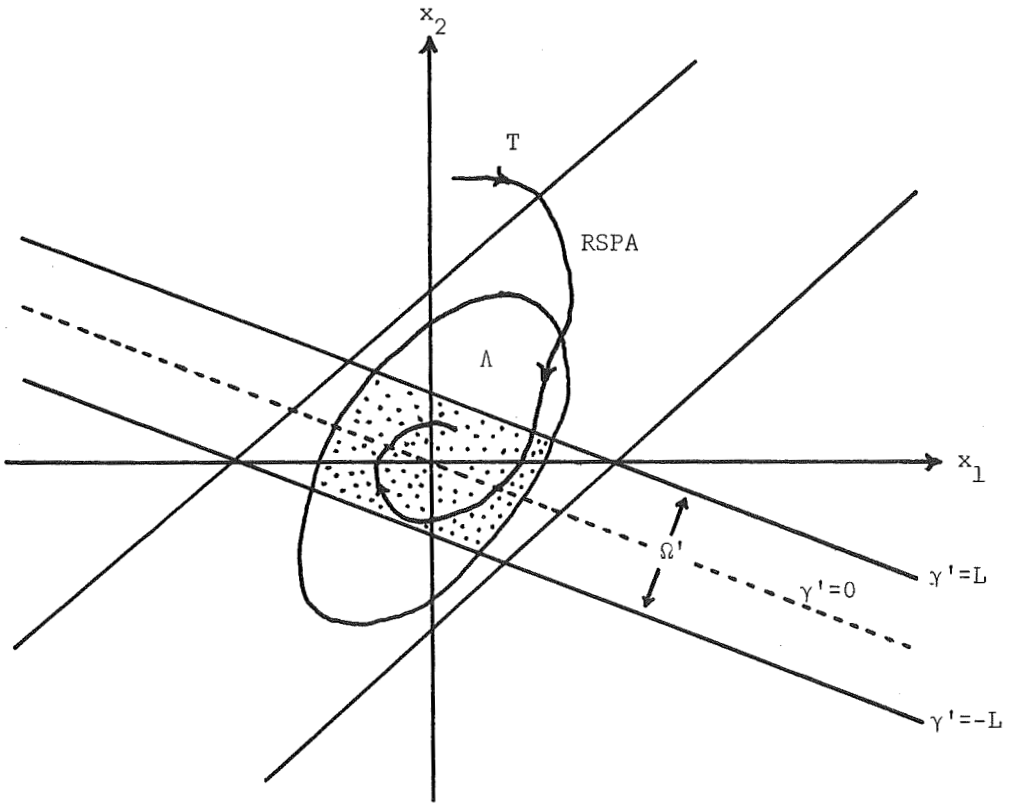

Figure 3.7
The Case Λ Contained in RSPA

trajectory T, enters Λ it must approach Ω' monotonically until it enters Ω'. Once it enters Ω' it must not necessarily approach the switching plane $\gamma = 0$ monotonically because in Ω' imperfection can destroy the property of RSPA. Paramount is the fact that once the trajectory enters

the portion of Ω' contained in Λ, indicated by the shaded region in Figure 3.7, it remains in Ω' for all subsequent time. The bound calculation scheme of Chapter V therefore applies to (3.10) if Λ, (3.26), is contained in RSPA (3.27). The condition that guarantees this is given in (2.26) to be

$$[\beta \underline{\alpha}'^{T} \underline{c}']^2 \geq M_1 M_3 / M_2 \tag{3.28}$$

where M_1 and M_2 are as in (3.26) and M_3 is the largest eigenvalue of $[P'^{-1} A'^{T} \underline{\alpha}' \underline{\alpha}'^{T} A']$.

The importance of (3.28) is best appreciated by considering the situation that results when Λ is not entirely contained in RSPA as sketched in Figure 3.8. The trajectory, T, demonstrates that at

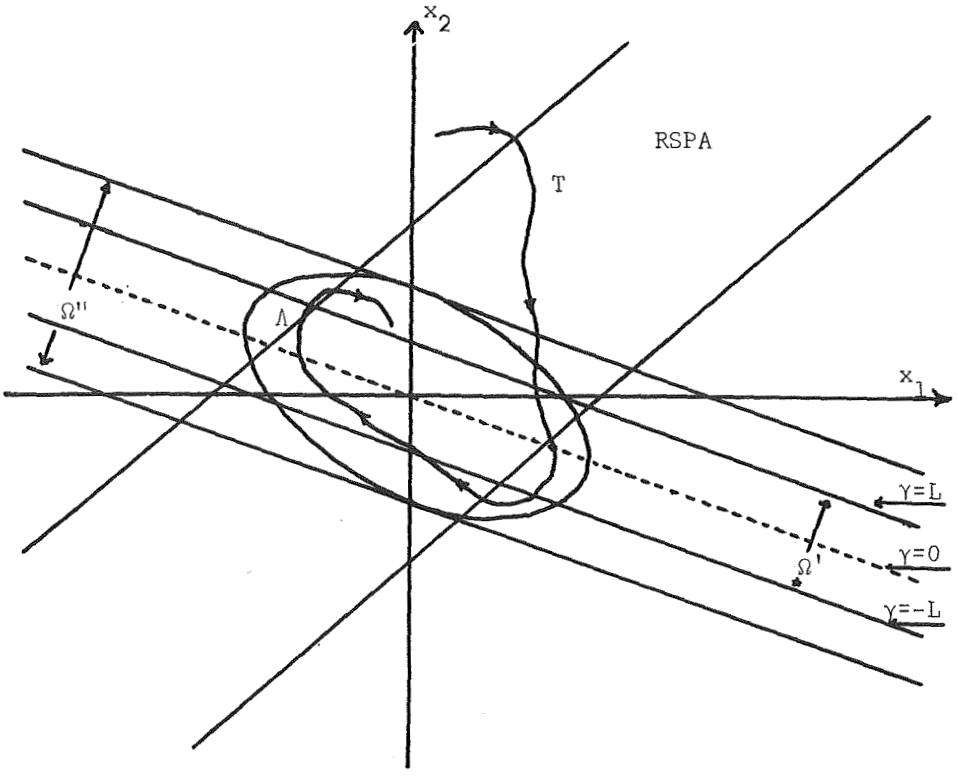

Figure 3.8

The Case Λ Not Contained in RSPA

points in Λ not in RSPA, T can move away from the switching plane and

thus destroy the property of monotonic approachment of Ω'. For the bound calculation, a much larger region Ω'' would have to be used, for this is the smallest invariant region of imperfect control. This would lead to a larger bound estimate which would not approach zero in the absence of imperfection.

It should be emphasized that (3.28) is only important because of a bound calculation technique that will be used to evaluate the affects of imperfection. Specifically, it guarantees that the technique results in a bound that approaches zero in the limit as imperfection, or equivalently, L goes to zero.

The augmented system design is completed with the development of Chapter V.

IV The Model-Reference Control Problem

When confronted with the problem of controlling a plant which is imperfectly identified, it is often necessary to employ extensive simulation studies in order that desired performance is guaranteed. Although many approaches to solving this problem have been made, in particular along the lines of adaptive control, a well defined synthesis procedure cannot be said to have been defined. One approach to solving this problem involves the application of identification techniques. However, these methods require expenditure of time, and in many cases, if not ruled out by cost factors alone, are not reliable because the stability is not guaranteed due to the computation lag involved.

An alternative to this approach is to develop a control which guarantees stability over the range of parameter uncertainty involved. Although this solution to the problem will not be the most efficient, it may be justified in terms of cost, or simply because no other method is available. This method of control which has been discussed by several authors [1], [2], [3] depends upon the synthesis of a control law which guarantees stability by application of Liapunov's direct method. This is accomplished by means of a model-reference control system as characterized in Figure 4.1.

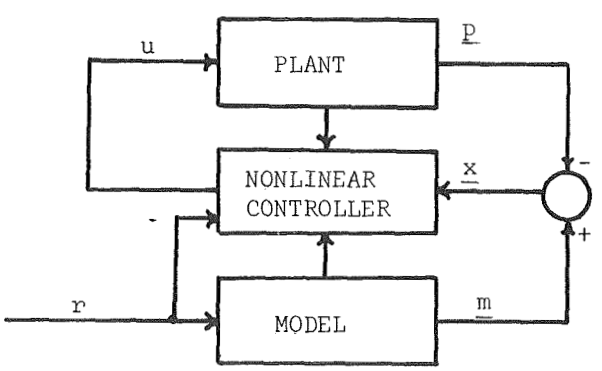

Model-Reference Controller

Figure 4.1

The object of the model-reference control scheme is to force the states, p_i, of a single-input, single-output, nonlinear, time-varying, n^{th}-order plant to track the states, m_i, of a linear, time-invariant n^{th}-order model as the model responds to some input. The main requirement on the control is one of stability. Stated in general terms, this requires that some measure of the offsets, x_i, between plant and model states, the tracking error, must either tend to zero in the limit with time (Asymptotic Stability) or eventually be contained within some small calculable bound (Lagrange Stability).

The main contribution of this thesis is an extension of previous work to allow filter states to be used in formulating the control law, thereby reducing noise content in the general design and moreover providing the designer with the opportunity to use filtered derivatives of measureable signals to approximate states that cannot be measured. In addition, it facilitates the evaluation of the affects of transducer dynamics which heretofore have been neglected.

Justification of the Relay Model

The essential problem can be related to an equation of the form

$$\dot{\underline{x}} = A\underline{x} - \beta(t)\ \underline{c}\ \mathrm{sgn}\ (\gamma(x)) \qquad (4.1)$$

where the stability matrix A and the input vector $\underline{c}$ are in phase variable form

$$A = \begin{vmatrix} 0 & 1 & & & \\ & 0 & 1 & & \\ & & 0 & 1 & \\ & & & \ddots & \ddots \\ & & & & 1 \\ -a_1 & - & - & - & -a_n \end{vmatrix} \quad , \underline{c} = [0 \ldots\ldots 1]^T \qquad (4.3)$$

$$0 \leq \beta(t) \leq 2L \qquad (4.4)$$

The signum function is defined to be

$$\text{Sgn}\ (\gamma) = \begin{cases} +1 \ ; \ \gamma > 0 \\ \sigma \ : \ \gamma = 0; \ -1 \leq \sigma \leq 1 \\ -1 \ ; \ \gamma < 0 \end{cases} \tag{4.5}$$

and the linear switching function is

$$\gamma = \underline{\alpha}^T \underline{x} = \sum_{i=1}^{n} \alpha_i x_i \tag{4.6}$$

where with no loss in generality we assume $\alpha_n = 1$. In (4.1) $\underline{x}$ represents the vector difference $\underline{m} - \underline{p}$, A could represent the linear model dynamics and $\beta(t)$ is equal to a sum of nonlinear, time-varying terms which, as a result of the relay controller, is always positive and as a consequence of the relay output level L is bounded by 2L.

That (4.1) is a proper representation of the controlled model-reference system can be seen by the following example. Figure 4.2 is the signal flow graph of a third-order nonlinear, time-varying plant having states p_i that are to track those of the stable linear, time invariant model reference m_i respectively. Ignorance of the plant is expressed in $g(\underline{p},t)$ and $c_p(t)$. The former contains non-linear terms and coefficients known only within bounds; the latter is bounded away from zero and known only within bounds.

The sign of the control, u, is that of the switching function $\gamma(\underline{x})$. The gain $M(\underline{x},\underline{p},r,t)$ in the designs of references [1] and [2] is generated in the nonlinear controller to form the magnitude part of the control. To satisfy plant saturation constraints it must be shown that M is less than some number L. In so doing, one guarantees that substitution of the constant L or M would give the same stability results. This is the motivation for the design of reference [3] where M = L and the nonlinear controller is essentially a relay.

The relevance of (4.1) to the system of Figure 4.2 becomes apparent through the equivalent signal flow represented in Figure 3. A property of the synthesis techniques of references [1], [2], [3] is that the signal at node a has the sign of $-\gamma$ and a magnitude bounded by 2L. Inasmuch as stability of the tracking is based on stability of the error states x_i then stability of the controlled model-reference system may be based on (4.1). This is in the spirit of theorem (2.1)

Before going further several points should be made concerning (4.1) and its relevance to the model-reference controlled system, inasmuch as the remainder of this chapter is based entirely on (4.1)

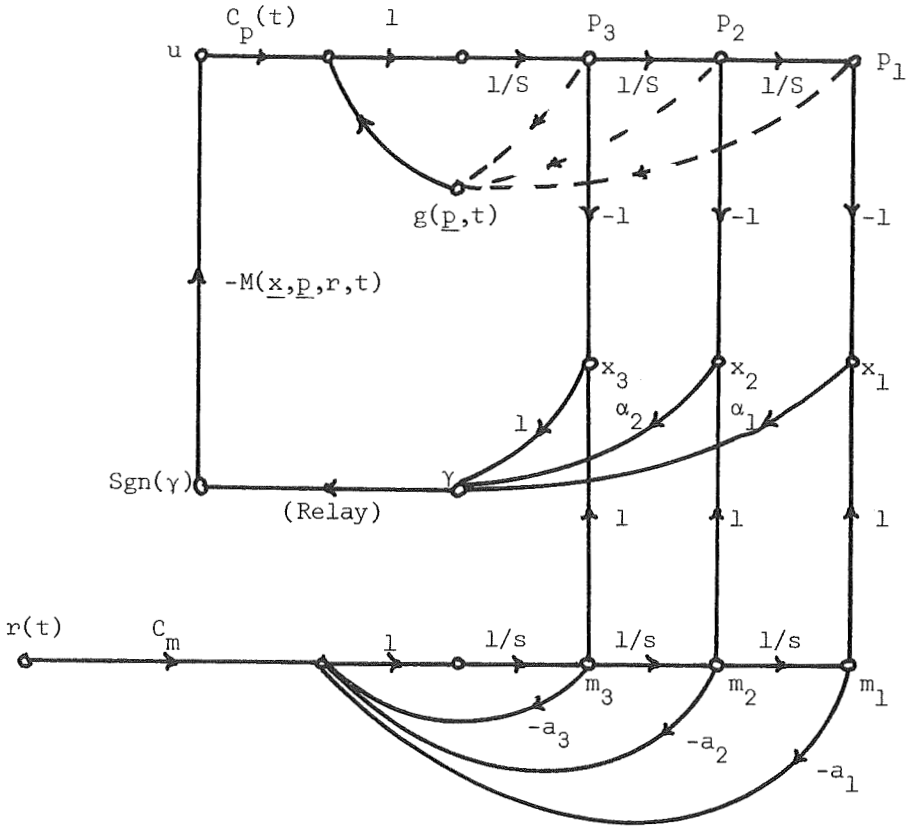

Third-Order Model Reference Controller

Figure 4.2

First, this relation is not the only one that could have been chosen. The important qualities that must be preserved by the second term on the right of (4.1) are that it must be bounded in magnitude and must take the sign of $-\gamma$. Another valid representation, for

example, would be the expression $c(t)\gamma(x)$ where $0 \leq c(t) \leq \infty$. The reason for the unboundedness of the time-variable gain $c(t)$, is explained by the second point.

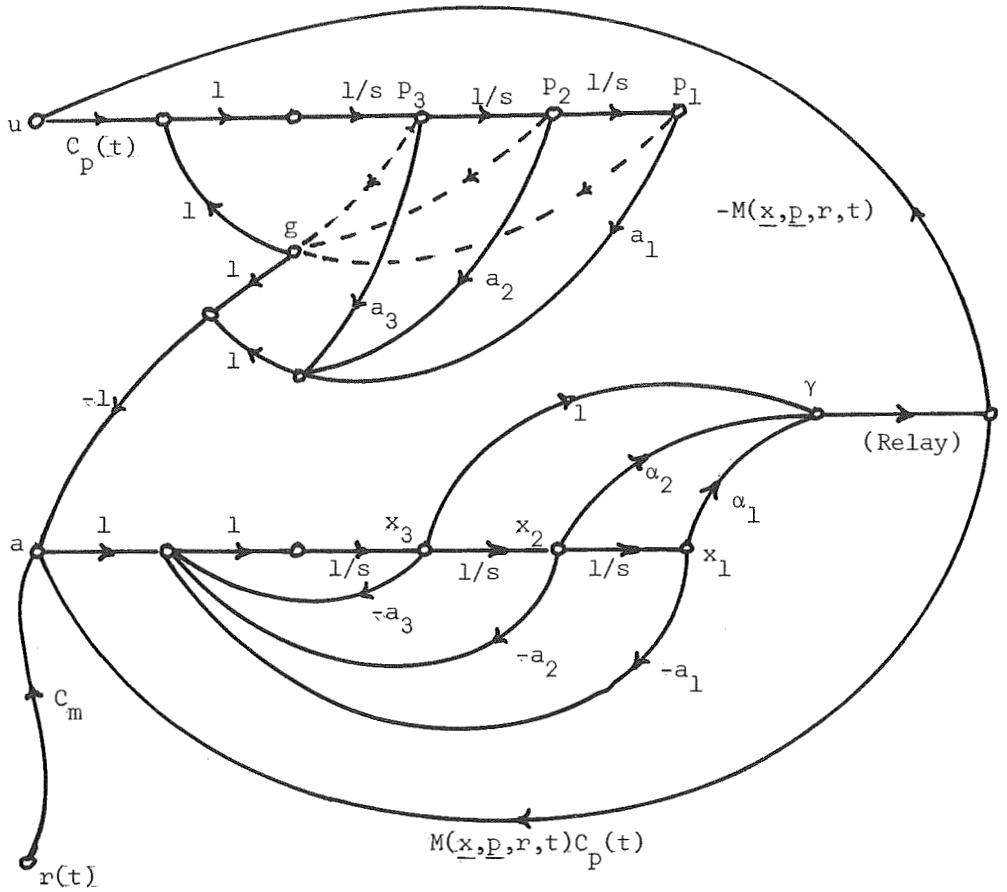

Equivalent Third-Order Model Reference Controller

Figure 4.3

Although the node a is bounded and takes the sign of $-\gamma(\underline{x})$, it is not necessarily zero when γ is zero. Thus, if a linear gain is to relate the two it must have infinite range. (Notice also that this property is present in (4.1) in the infinite slope of the Signum Function). It is this property which makes the stability analysis

of (4.1) so difficult.

The third point to be made is that, due to the presence of non-linear terms and time-variable coefficients known only within bounds very little can be implied about the signal a. This ignorance is translated to $\beta(t)$ in (4.1). Consequently, no definite statement can be made concerning the time derivative of $\beta(t)$. This also confounds the analysis problem.

Another point is that due to the ignorance in $\beta(t)$ the relay system (4.1) is capable of motions that may not be possible in the actual controlled system. This is due to parameter ignorance. Of paramount importance, however, is the fact that all possible motions of the controlled system are motions of (4.1), and therefore any properties that can be attributed to solutions of (4.1) apply also to those of the model-reference controlled system. Therefore, (2.1) applies here.

The last point is that having assumed stability conditions to be satisfied by the relay output level, L, or varying gain $M(\underline{p},\underline{x},r,t)$, the only design freedom that remains is the choice of the switching function $\gamma(\underline{x}) = \underline{\alpha}^T\underline{x}$.

The relevance of (4.1) to the controlled model-reference system has been demonstrated graphically. At the end of this chapter this is born out by a numerical example. The problem that remains is to obtain a design criteria for the case wherein the highest-order state, x_n, is not available for implementation of the switching function $\gamma(\underline{x})$.

Derivation of Filtered System

It was pointed out in Chapter III that the conventional Liapunov synthesis technique fails to give conditions for asymptotic stability of (4.1) that result in a γ which is independent of the highest-order state x_n. The technique of Chapter III cannot be applied to (4.1) because the augmented system transfer function would have time-varying zero locations and the Kalman theorem [6] used to derive theorem (2.14) would not apply. In the time domain this is born out by the fact that the (4.1) counterpart of (3.10) could not have a separable

gain $\beta(t)$ as is required by (2.14). This is a consequence of the ignorance of $\beta(t)$ in (4.1). Thus a new approach is required.

The solution proposed here is to pass the noisy measurements of the highest-order available states through filtered-derivative circuits to be used in place of the unavailable states. This is considered equivalent to passing the unavailable states along with the differentiated noise through the respective filters. This equivalence makes the analysis also apply to the transducer dynamics problem, inasmuch as transducers act as filters for the measured states.

In what follows, the case x_n unavailable is treated, for it is the elimination of this particular state that presents the greatest challenge. This is due to the fact that it can only be obtained by differentiating a lower-order-derivative state. The problem of eliminating any other state is synthetic in the sense that it could be obtained by integrating another state. Extension to the case of r unavailable highest-order states is straightforward.

In a situation where the highest-order-derivative state x_n is not accessible but is required for asymptotic stability, a reasonable solution is to use a filtered derivative of x_{n-1} in place of x_n. Choice of filter dynamics would be based on some knowledge of measurement noise statistics. In this case, the filter transfer function would have a denominator polynomial of order two or higher to provide adequate low pass filtering of white noise encountered in the measurement of x_{n-1}. In the case of colored noise a first-order filter might suffice but for generality we consider a second order filter. For purposes of this discussion such a filter will be represented by

$$c_2\ddot{x}_{n+1} + c_1\dot{x}_{n+1} + x_{n+1} = \dot{x}_{n-1} \tag{4.7}$$

This can also be expressed as

$$c_2\ddot{x}_{n+1} + c_1\dot{x}_{n+1} + x_{n+1} = x_n, \tag{4.8}$$

because in the phase-variable structure, $\dot{x}_{n-1} = x_n$. However,(4.7) is written to indicate that the state x_{n-1} is the input to the filter rather than x_n as indicated in (4.8). Accordingly the derivative of noise encountered in the measurement of x_{n-1} would appear on the right

side of (4.8).

An augmented system results when the filter (4.8) is incorporated into the original system (4.1), that is, when the state x_{n+1} is used in place of x_n in the switching function (4.6). It can easily be shown that the stability analysis of this augmented system is hindered in much the same manner as was that of (4.1).

Even though asymptotic stability cannot be guaranteed in the augmented system it is reasonable to expect that the filter could be chosen so as to minimize the ultimate state bound that may result. Toward this end we consider the term

$$e = x_n - x_{n+1}. \tag{4.9}$$

It is this filter error that distinguishes the augmented system from the original system (4.1). In fact, for the following discussion it is convenient to express the augmented system as

$$\dot{\underline{x}} = A\underline{x} - \beta(t)\ \underline{c}\ \mathrm{Sgn}\ (\underline{\alpha}^T\underline{x} - \alpha_n e). \tag{4.10}$$

The problem that remains is to choose the switching function coefficients $\alpha_1, \alpha_2 \ldots \alpha_n$ and filter constants c_1, c_2 to minimize the ultimate bound on solutions of (4.10).

One solution is to choose $\underline{\alpha}$ so that (4.10) is asymptotically stable for the case $e \equiv 0$. Then treating the term $\alpha_n e$ as switching function imperfection, a realistic bound can be determined by means of the development of Chapter V. Such a bound would only be valid if motion of the imperfect system were confined to the region of imperfect control. Since this is not true in general, an alternate design is desirable.

In the following section a new design technique is developed for which the technique of Chapter V applies to any initial condition. A natural switching function is shown to guarantee that solutions of (4.10) will monotonically approach a hyperplanar region, Ω, parallel to and centered about the switching plane. By nature of the fact that $\underline{x}$ will eventually enter Ω and will remain there for all subsequent time, the bound technique of Chapter V applies directly. This bound is proportional to the width of Ω or equivalently the eventual bound on $|\gamma|$ which in turn is based on worst-case magnitudes of filter

error and filtered measurement noise. The trade-off that exists between the effects of these two bounds is discussed in the example which concludes this chapter.

Natural Switching Function Design

Paraphasing a theorem of Lasalle's [8], it is possible to obtain asymptotic stability with the use of a semidefinite Liapunov function providing: a) that the function approaches zero asymptotically and b) that motion on the zero manifold is asymptotically stable to the origin. In terms of the problem at hand where linear switching is employed, asymptotic stability could be achieved if sufficient conditions could be found to guarantee that the switching function approaches zero monotonically and that motion on the switching hyperplane is asymptotic to the origin. It has been shown in (2.35) that choice of what is called a natural switching function guarantees both conditions.

Thus according to (2.35) asymptotic stability of (4.1) will result if A has at least one real, distinct eigenvalue $-\lambda$ and the switching function coefficient vector $\underline{\alpha}$ is chosen as the corresponding eigenvector of A^T. That is, $\underline{\alpha}$ satisfies the relation

$$A^T\underline{\alpha} = -\lambda\underline{\alpha}. \tag{4.11}$$

The natural switching function design for the case of an n^{th}-order system is only possible when A^T and equivalently A has at least one distinct real eigenvalue. For the case of $m \leq n$ simple roots there are m possible natural switching functions. This design has several merits. The most important will now be demonstrated.

Having established asymptotic stability in the absence of filter error, the problem remains to obtain a realistic estimate of the bound on $\underline{x}$ due to a given filter. The method to be employed here is to show that the state vector is confined to a certain neighborhood of the switching plane. Then the bound estimation technique may be employed. The problem therefore is to obtain a realistic bound on $\gamma(\underline{x})$, thus guaranteeing that $\underline{x}$ is contained in a hyperplanar region centered about and parallel to the switching plane. The system with filter error is represented by

$$\dot{\gamma} = -\lambda\gamma - \beta(t) \cdot \mathrm{Sgn}\,(\gamma - e). \tag{4.12}$$

The following discussion is based on the fact that magnitude of γ will be decreasing as long as

$$|\gamma| \geq |e| . \tag{4.13}$$

It becomes apparent that the bound on $|e|$ becomes an upper bound on $|\gamma|$. Minimization of the bound is therefore simply based on the minimization of $|e|$. The object then in obtaining an upper bound on $|e|$ is to determine the largest value of $|\gamma|$ that can result.

The natural switching-function system is described by the following set of equations and corresponding flow graph, Figure 4.4. This is a collection of equations (4.6), (4.9), (4.10) and (4.12).

$$\begin{aligned}
\dot{x}_1 &= x_2 \\
\dot{x}_2 &= x_3 \\
&\vdots \\
\dot{x}_{n-1} = x_n &= -\sum_{i=1}^{n-1} \alpha_i x_i + \gamma \\
\dot{x}_{n-1} &= x_{n+2} \\
c_2 \dot{x}_{n+2} &= -x_{n+1} - c_1 x_{n+2} - \sum_{i=1}^{n-1} \alpha_i x_i + \gamma \\
\dot{\gamma} &= -\lambda\gamma - \beta(t)\ \mathrm{Sgn}\ (\gamma - e) \\
e &= x_n - x_{n+1}
\end{aligned} \tag{4.14}$$

The filter error responds to initial conditions of all integrator outputs and to the relay output. However it is the driven response that is of interest here for it is this response that prevails to possibly affect an eventual bound. To find an upper bound on the largest $|e|$ that can be reached, the system is initiated at $\underline{x} = \underline{0}$ and the relay is allowed to switch, regardless of its switching function, so that $|e(t)|$ is maximized. Note that the system in Figure 4.4 does not

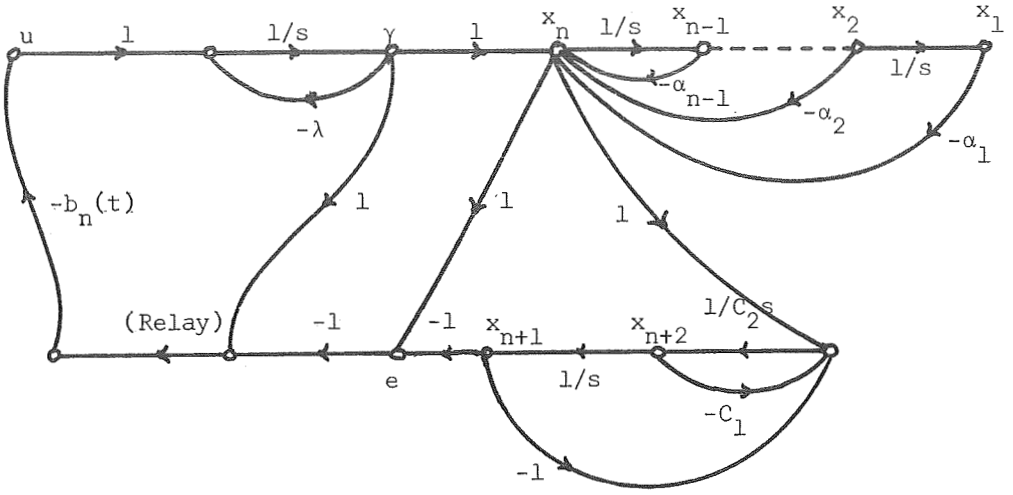

Natural Switching Function System

Figure 4.4

involve plant parameters.

To achieve the optimization, it is convenient to use the transfer function relating the nodes u and e in the absence of the non-linear feedback path. This takes the form

$$\frac{E(S)}{U(S)} = H(S) = \frac{S^n(C_2S + C_1)}{(S+\lambda)(S^{n-1}+\alpha_{n-1}S^{n-2} + \text{---} \alpha_2S + \alpha_1)(C_2S^2 + C_1S + 1)} \quad (4.15)$$

for which the inverse transform h(t) obviously exists. It is important to note that the term $1/(S+\lambda)(S^{n-1} + \alpha_{n-1}S^{n-2} + \text{---} + \alpha_1)$ relates u to x_1 and therefore the roots of this polynomial are identical with the eigenvalues of A. That is to say

$$(S+\lambda)(S^{n-1} + \alpha_{n-1}S^{n-2} + \text{---} \alpha_2S + \alpha_1) = \det(IS-A) \quad (4.16)$$

Also in (4.15) the S^{n-1} part of the numerator relates x_1 to x_n. The remaining term relates x_n to e by the filter equation (4.9) and the relation $e = x_n - x_{n+1}$,

$$\frac{E(S)}{X_n(S)} = \frac{S(C_2S + C_1)}{(C_2S^2 + S_1S + 1)} . \quad (4.17)$$

According to (2.58) the largest $|e(t)|$ that can result for $|u(t)| \leq 2L$ is

$$|e|_{max} = 2L \int_0^\infty |h(\tau)| \, d\tau. \tag{4.18}$$

With this result, the minimization of $|e|$ and consequently of $|\gamma|$ and of the eventual bound on $\underline{x}$ can be discussed.

One method of reducing e beyond the result of (4.18) involves the fact that the behavior required of $\beta(t)$ and of the relay, or equivalently, of u(t), to produce the maximum $|e|$ would most likely produce a γ that is larger than e in magnitude. If a second interation were performed wherein this constraint were placed on γ or equivalently on u(t) it is certain that a smaller $|e|$ would result. This could possibly converge through several interations to a much smaller value and possibly zero. However, the optimal problem involves a state-space constraint and its solution has not been determined.

It might be thought possible to apply the optimal technique used in obtaining (4.18) to the transfer function relating the transforms of γ and e, namely, $(S+\lambda)\, H(S)$. However inasmuch as this has numerator and demoninator of equal order it will never occur that $|e|$ would be less that $|\gamma|$.

It will now be shown for the case when A has a large negative eigenvalue that $|e|_{max}$ will be correspondingly small. When this is not the case it is shown that the filter (4.8) can be chosen to make $|e|_{max}$ in (4.18) arbitrarily small at the expense of admitting noise encountered in the measurement of x_{n-1} into the switching function. The trade-off of γ-bound due to filter error and filtered noise will also be pointed out.

Bound on $|\gamma|$

With the help of Figure 4.4 it is seen, since $|u| \leq 2L$, that the largest $|\gamma|$ which can occur is $2L/\lambda$. Clearly, if A were to have a real eigenvalue with very large negative value, the hyperplane perpendicular to its corresponding eigenvector could be chosen as a natural switching plane. This situtation offers two advantages.

The resulting bound on γ would be very small and, by nature of the solution of (4.12) $|\gamma|$ would tend to converge faster from some initial condition to the bound $2L/\lambda$ than would be the case with smaller values of λ. This result agrees with intuition in that the lack of highest derivative information should not be so serious in a system which could be approximately represented by a lower-order system.

It will now be shown that when A does not have this property, the filter can be chosen so that the bound on $|e|$ and therefore on $|\gamma|$ can be designed to be arbitrarily small. If the transfer function of the general filter in (4.8) is replaced by a second-order filter with simple real poles so that

$$\frac{x_{n+1}(S)}{x_n(S)} = \frac{1}{(\tau_1 S + 1)(\tau_2 S + 1)}, \tag{4.19}$$

that is if $C_2 = \tau_1\tau_2$ and $C_1 = \tau_1 + \tau_2$, then the transfer function relating x_n to e is

$$\frac{E(S)}{x_n(S)} = \frac{S[S + (\tau_1 + \tau_2)/\tau_1\tau_2]}{(S + 1/\tau_1)(S + 1/\tau_2)} \tag{4.20}$$

If τ_1 is chosen much less than τ_2 we have

$$\frac{E(S)}{x_n(S)} = \frac{S}{(S + 1/\tau_2)}; \quad \tau_1 << \tau_2. \tag{4.21}$$

In light of this the transfer function relating u and e from (4.9) becomes

$$\frac{E(S)}{U(S)} = H(S) \frac{S^n}{\det(IS - A)(S + 1/\tau_2)}, \tag{4.22}$$

which can be expressed as shown in Figure 4.5.

A consequence of the magnitude constraint $|u| \leq 2L$ and the constraint $\tau_2 << \tau_1$ is that

$$|\xi| \leq 2\tau_2 L \tag{4.23}$$

Inasmuch as e is the output of a realizable filter having all roots with negative real parts it follows that e is bounded in proportion to

the filter input ξ. Thus e approaches zero with τ_2. However, to reduce the bound on $|e|$ and $|\gamma|$ in this way, τ_2 must be made small and as a result $S = 1/\tau_2$ becomes a far-out pole. Furthermore, the filter pole at $S = 1/\tau_1$ is even farther out by the assumption $\tau_1 << \tau_2$. These far-out poles admit high frequency measurement noise to the switching function. Treating this noise as an additive signal in the switching function and assuming a magnitude constraint on the noise $|n(t)| \leq N$ it follows that the sign of γ and therefore the relay output cannot be affected if $|\gamma| \geq N$. Thus Sgn $\gamma \neq$ Sgn $(\gamma - e)$ only if $|\gamma| < N$.

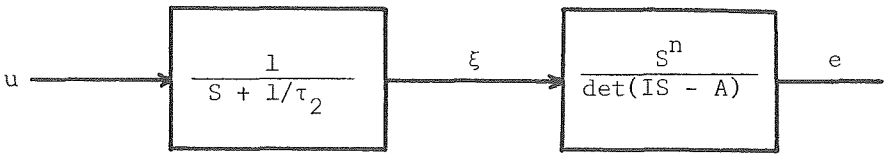

Equivalent Expression of (4.22)

Figure 4.5

Due to the fact that the switching line is approached monotonically in absence of switching function imperfection, and since n(t) can only cause imperfection when $|\gamma| < N$, it follows that a bound on $|\gamma|$ results due to noise alone. This bound is $|\gamma| \leq N$.

It becomes apparent that the cost of choosing a wide-bandwidth filter to decrease the bound on $|\gamma|$ caused by filter error is that a greater bound on $|\gamma|$ due to the presence of high frequency noise may result. The filter would have to be based on some knowledge of the measurement noise in any particular application. To further evaluate the trade-off that exists in the absence of information about the number N, statistical properties of the bound on $|\gamma|$ due to noise could be used rather than absolute maximum values as were used in this instance.

A further advantage of the natural switching function design that becomes apparent here is that the bound on $|\gamma|$ due to both filter error and filtered noise is simply the sum of the bounds due to each acting separately. The reason is that each is based upon imperfection in the switching function and this is an additive quantity. That is to say, if filtered noise n(t) bounded in magnitude by N, and filter error e bounded in magnitude by E, are both present in the implemented signal γ, imperfect control can result only in the state space region denoted by

$$\Omega_{NE} = \{\underline{x}: |\gamma(\underline{x})| \leq N + E\}. \tag{4.24}$$

This is termed the "region of imperfect control". This region for the case of filter error or filtered noise acting alone is

$$\Omega_E = \{\underline{x}: |\gamma(\underline{x})| \leq E\}. \tag{4.25}$$

and

$$\Omega_N = \{\underline{x}: |\gamma(\underline{x})| \leq N\}. \tag{4.26}$$

respectively.

Having established the region of imperfect control for (4.10) and thus for (4.1), and having guaranteed by the natural switching function design that once $\underline{x}$ enters Ω_{NE} it will remain in this region for all subsequent time, it is possible to determine an eventual bound on the states x_i by employing a technique reported in [4]. This is the subject of the next chapter.

Design Example

The concepts developed above will now be applied to the roll attitude control of the aircraft sketched in Figure 4.6a. In accordance with the block diagram representation of the plant given by Figure 4.6b, the control signal u(t) is integrated through the aileron hydraulics to produce an aileron deflection $\delta(t)$. This deflection, by nature of the constant velocity of the aircraft in a uniform medium, results in a roll rate $\dot{\phi}(t)$ which is related to the integral of $\delta(t)$ by the coefficient a. The roll rate is dampened according to the parameter c due to the wings rolling through the medium. Geometry then

gives $\phi(t)$ as the integral of $\dot{\phi}(t)$.

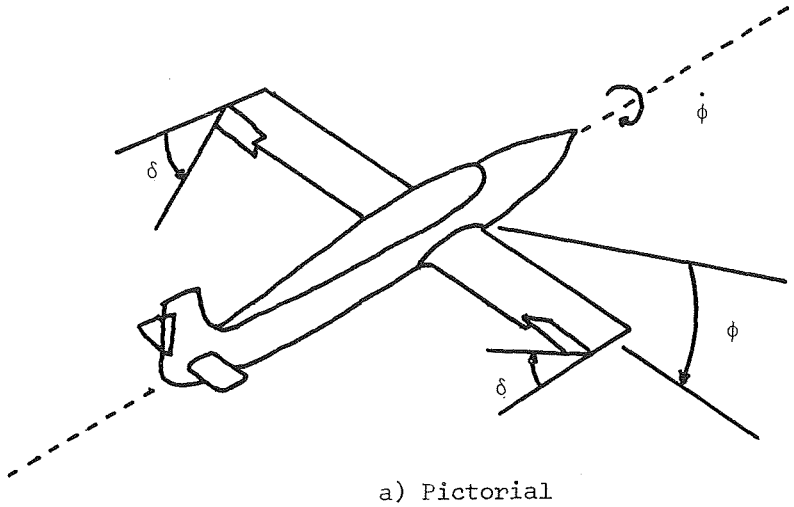

a) Pictorial

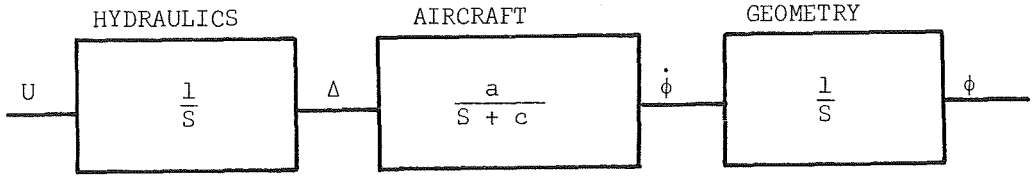

b) Block Diagram

Roll Attitude Control Example

Figure 4.6

At this point, control of the roll angle would be straightforward if the parameters a and c were known. However, both are inversely related to J_r, the moment of inertia of the aircraft about its roll axis. For a typical aircraft with fuel stored in the wings, or in the case of a more modern aircraft which has the capability of changing wing angle relative to the fuselage, J_r is a time-variable quantity. Furthermore, the affects of sloshing could possibly cause J_r to be known only within bounds. It is this sort of parameter ignorance that motivates the designer to consider the model-reference technique. However, to use this technique, the plant must first be transformed into phase-variable

form.

The equivalent phase-variable form of the plant is given in Figure 4.7 along with that of the desired model. The object is to develop a bounded control u(t) which will make the plant states follow the respective model-states as the latter respond to the roll angle command r(t).

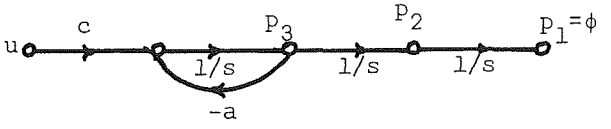

a) Plant

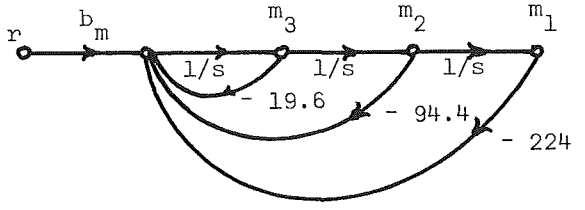

b) model

Phase-Variable Representation of Plant and Model

Figure 4.7

Before preceeding with the design it is interesting to note that this example illustrates an important point commonly found in practical designs. The highest-order plant state p_3 is not obtainable from a primary measurement. Unlike the states p_1 and p_2 which can be measured with an angular gyro and an angular rate gyro respectively, p_3 can only be obtained as a linear combination of $\delta(t)$ and $\dot{\phi}(t)$. However, the relative weighting is determined by the coefficients a(t) and c(t) which are not known. For this reason, the state p_3 is assumed to be unavailable and this necessitates the use of the reduced-state model-reference

design developed in this chapter.

Proceeding with the example, the plant and model are expressed in the state equations

$$\begin{aligned} \dot{p}_1 &= p_2 \\ \dot{p}_2 &= p_3 \\ \dot{p}_3 &= -a(t)\, p_3 + c(t)u \end{aligned} \tag{4.27}$$

$$\begin{aligned} \dot{m}_1 &= m_2 \\ \dot{m}_2 &= m_3 \\ \dot{m}_3 &= -224m_1 - 94.4m_2 - 19.6m_3 + 230r. \end{aligned} \tag{4.28}$$

At this point, ranges for the unknown parameters are assumed to be

$$\begin{aligned} 0.5 \leq a(t) \leq 1.0 \\ 50.0 \leq c(t) \leq 100.0 \end{aligned} \tag{4.29}$$

and it is assumed that plant saturation constraints demand that

$$|u| \leq 1. \tag{4.30}$$

By defining the error states

$$x_i = m_i - p_i, \quad i=1,2,3 \tag{4.31}$$

the error state equations are

$$\begin{aligned} \dot{x}_1 &= x_2 \\ \dot{x}_2 &= x_3 \\ \dot{x}_3 &= -224x_1 - 94.4x_2 - 19.6x_3 - f \end{aligned} \tag{4.32}$$

where

$$f = 224p_1 + 94.4p_2 + (19.6 - a(t)p_3 - 230r + c(t)u(t)) \tag{4.33}$$

Employing the relay design philosophy of Lindorff [3] the plant input constraint (4.30) is met by assuming

$$u(t) = \text{Sgn}\,[\gamma(\underline{x})] \tag{4.33}$$

where

$$\gamma(\underline{x}) = \alpha_1 x_1 + \alpha_2 x_2 + x_3 \tag{4.34}$$

Choice of this control makes it possible for the sign of u(t) to determine the sign of f(t). Corresponding to the magnitude constraint on u(t) and a class of command inputs, a region of initial

conditions on $\underline{p}$ and $\underline{m}$ can be found such that for all subsequent time u dominates the sign of f. Calculation of this region is somewhat tedious and is the subject of other research [12]. Paramount is the fact that its existence is dependent on asymptotic stability of (4.32).

It will now be convenient to express f(t) in a different form. The fact that f(t) has the sign of u(t), and thus of $\gamma(\underline{x})$, implies the inequalities

$$c(t)\, u(t) \geq f(t) - r(t)\, u(t),\ u = +1$$
$$c(t)\, u(t) \leq f(t) - r(t)\, u(t);\ u = -1 \tag{4.35}$$

which together imply

$$|f(t)| \leq 2|c(t)|. \tag{4.36}$$

This information concerning the magnitude and sign of f(t) permits it to be represented as

$$f(t) = b_3(t)\ \text{Sgn}\ \gamma \tag{4.37}$$

where in view of the limits assumed on c(t), (4.29), the variable $b_3(t)$ is bounded according to

$$0 \leq b_3(t) \leq 200. \tag{4.38}$$

As a consequence of (4.37), the model-reference control system (4.32) can be investigated by the system

$$\dot{\underline{x}} = A\underline{x} + \underline{b}(t)\ \text{Sgn}\ \gamma(\underline{x}) \tag{4.39}$$

where

$$A = \begin{vmatrix} 0 & 1 & 0 \\ 0 & 0 & 1 \\ -224 & -94.4 & -19.6 \end{vmatrix}, \quad \underline{b}(t) = \begin{vmatrix} 0 \\ 0 \\ b_3(t) \end{vmatrix}.$$

The system (4.39) will now be used as a model for (4.32) in the sense of the modelling theorem (2.1). This development illustrates algebraically what was illustrated graphically in Figures 4.2 and 4.3; that is that (4.1) represents the general model-reference control system.

To continue with the design example, a switching function must be chosen so as to guarantee asymptotic stability of (4.39). This is essential to the development because bounds on the solution of (4.39) due to various types of imperfection will be established and used

according to (2.1) as bounds on solutions of the model-reference control system (4.32). Inasmuch as A has one real eigenvalue, λ=14, a natural switching function may be chosen as a solution to the equation (4.11). rewritten here as

$$A^T\underline{\alpha} = -14\underline{\alpha}. \tag{4.40}$$

This results in $\alpha_1 = 16$ and $\alpha_2 = 5.65$, thus

$$\gamma = 16\, x_1 + 5.65\, x_2 + x_3. \tag{4.41}$$

As shown earlier, the fact that A is a stability matrix guarantees that this natural switching function will cause (4.39)to be asymptotically stable.

What remains is to determine estimates of bounds that will occur due to

(a) the use of a filtered derivative of x_2 in place of x_3 in the switching function,

(b) magnitude-limited, filtered, additive noise in the switching function and

(c) the use of an imperfect switching element in place of the ideal signum function.

In all cases a second-order filter having transfer function

$$1/(\tau S+1)(10\tau S+1) \tag{4.42}$$

will be used, and comparisons will be made between estimated bounds based on (4.39) and actual bounds measured on (4.32). All three cases are illustrated in Figure 4.8.

Case (a)

In case (a) the filter error e, defined as the difference between x_3 and the filtered derivative of x_2, is related to the node u(t) by (4.15) which in this case becomes

$$\frac{E(S)}{U(S)} = H_a(S) = \frac{S^2(10\tau^2 S + 11\tau)}{(S+14)(\tau S+1)(10\tau S+1)(S^2+5.6S+16)} \tag{4.43}$$

Inasmuch as $u(t) \leq 200$, a bound on $|e|$ can be obtained by use of (2.58) rewritten here as

$$|e_a|_{max}(\tau) \leq 200 \int_0^\infty |h_a(\sigma)|\, d\sigma \tag{4.44}$$

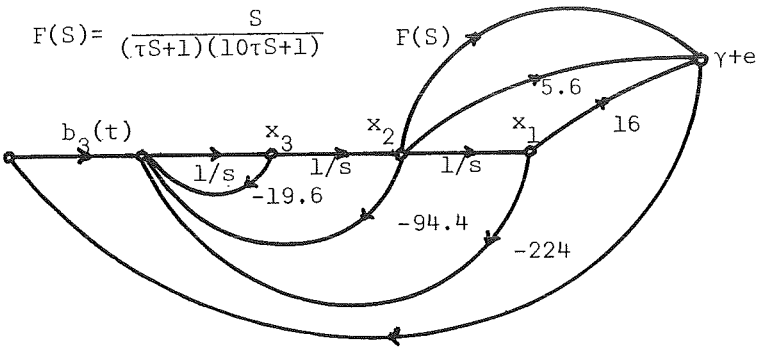

a) Filter Error

n(t) Gaussian White Noise
Mean: 0.
Variance: 1.

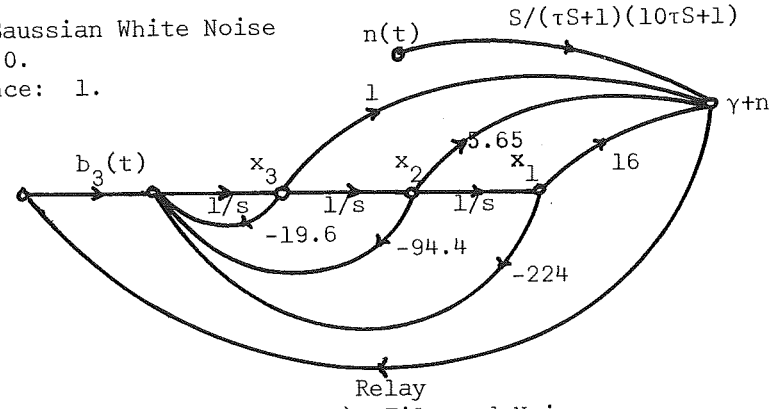

b) Filtered Noise

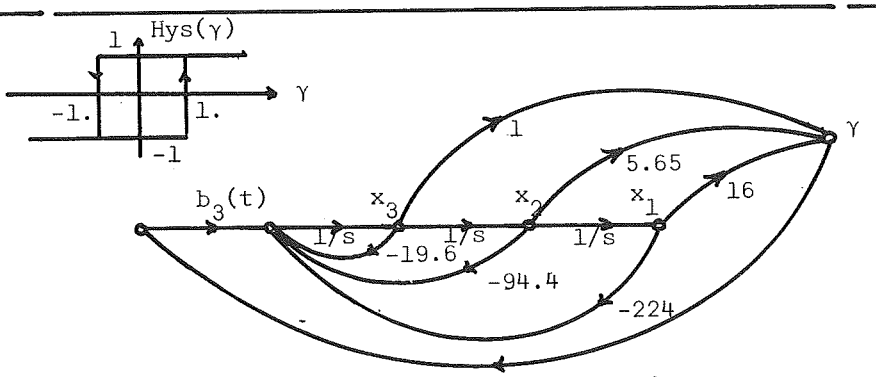

Hysteresis Function

c) Imperfect Switching Element

Three Cases of Imperfection Considered

Figure 4.8

where $h_a(t)$ is the impulse response of $H_a(S)$. The calculation of (4.44) was carried out digitally for a range of values of τ. Results are tabulated in Figure 4.9. These values provide the estimate of the width of the region of imperfect control as defined by (4.25).

τ	.01	0.1	1.	10.
$\|e_a\|_{max}$	15.8	1.58	.158	.0158
$\|e_b\|_{max}$	8.32	11.4	10.38	10.34

Bounds Estimated For Systems of
Figures 4.8a and b.

Figure 4.9

Case (b)

In this case switching function error, e(t), is defined simply as the filtered noise, assuming the noise n(t) is limited by 1 in magnitude. The filter relating the two is

$$\frac{E(S)}{N(S)} = H_b(S) = \frac{S}{(\tau S+1)(10\tau S+1)} \tag{4.45}$$

and corresponding to case (a),

$$|e_b|_{max}(\tau) = \int_0^\infty |h_b(\sigma)|d\sigma. \tag{4.46}$$

These values were computed and are tabulated in Figure 4.9. At this point, Figure 4.9 could be used to choose a best filter in terms of the predicted bounds on $|\gamma|$.

Case (c)

As pointed out earlier, the hysteresis element depicted in Figure 4.8 gives perfect control for the case in which $|\gamma| > 1$. Therefore the estimated region of imperfect control is given by $|\gamma| \leq 1$.

Computer Simulation

Digital computer simulation of (4.32) was made with

$$a(t) = \frac{1}{2}(1 + e^{-t/5})$$

$$b(t) = 100\ a(t)$$

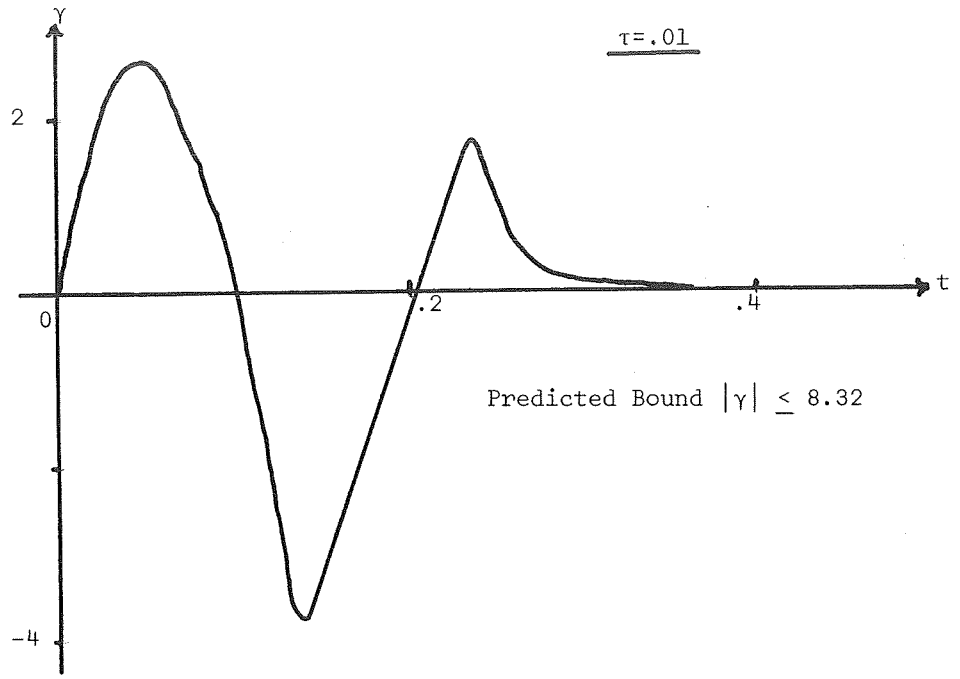

a) Filter Error

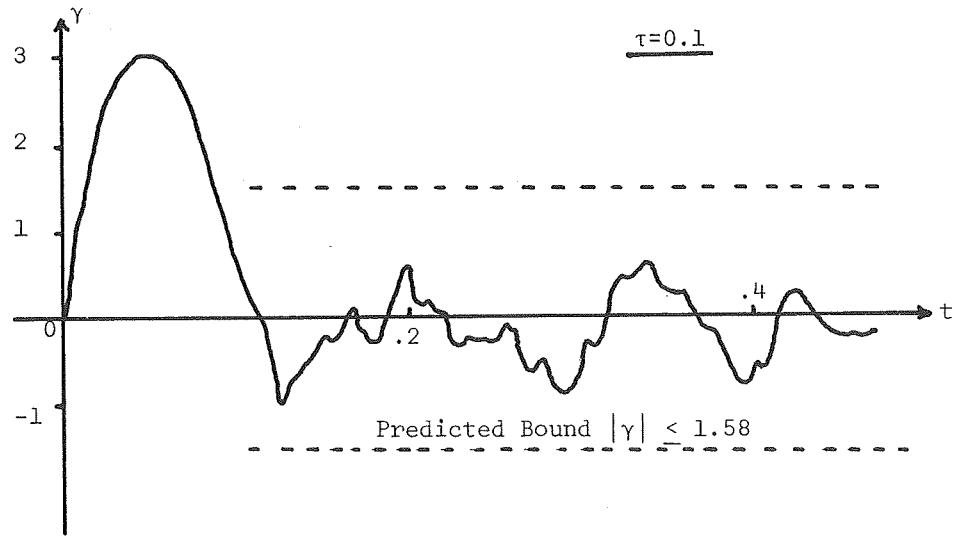

b) Filtered Noise

Simulation Results for Cases a and b

Figure 4.10

$$r(t) = 1$$
$$\underline{x}(0) = \underline{0}. \tag{4.47}$$

In many separate runs the same imperfections used in cases (a) and (b) were built into (4.32), and data was taken for several values of τ. The width of the region of imperfect control was determined from the data by determining the largest value of γ that was achieved in each computer run. These values are plotted in Figure 4.9 for purposes of comparison. Using the IBM Continuous System Modelling Program, data was taken for the three cases represented in Figure 4.8. One example of Case a is plotted in Figure 4.10a. The peak value of $|\gamma|$ that occurred for $\tau = 0.01$ was 4.03 and the maximum predicted was 8.32. This result is realistic. However, it is important to note that after transient affects subsided, the actual $|\gamma|$ was much less than the predicted bound. This is to be expected since the bound was based on a worst case situation.

Simulation of Case b is illustrated in Figure 4.10b for the case $\tau = 0.1$. After transients, $|\gamma|$ was less than .75 whereas the predicted bound was 1.58. The initial transient exceeded this bound for a short time due to the fact that the relay output was not sufficiently large to guarantee that u dominate the sign of f as assumed. This illustrates

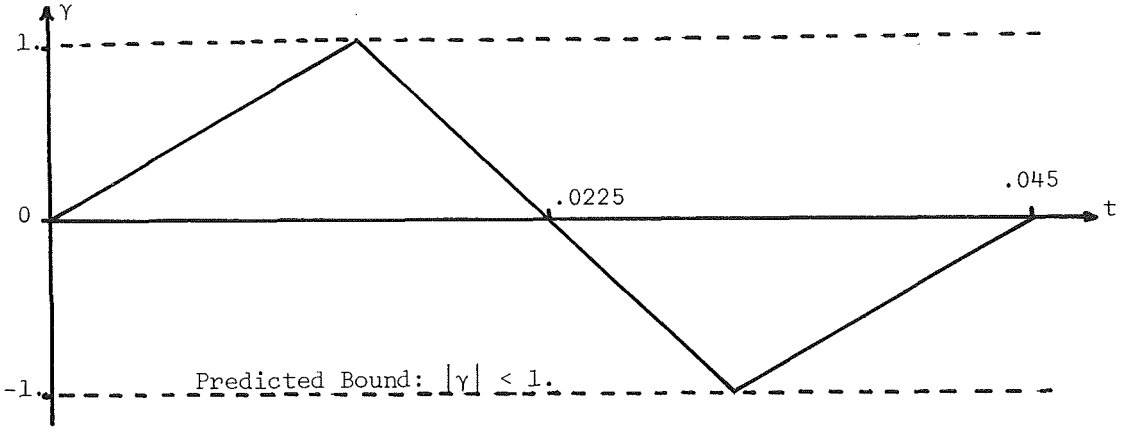

Limit Cycle of $\gamma(t)$ for Case c

Figure 4.11

the importance of the previously mentioned research concerning stability regions of model-reference controlled systems [12]. The fact that this was not considered in this design allowed for the possibility of this overshoot.

Simulation of Case c gave the least conservative results. The estimated $|\gamma|$ was 1 and that which occurred was 0.997. A limit cycle occurred. This resulted in $\gamma(t)$ as plotted in Figure 4.11. This figure illustrates the power of the natural switching function design. It illustrates that the state vector was trapped in the region of imperfect control.

It is convenient to use the state-bound calculation scheme of Chapter 5 to complete this example. Up to this point, the bounds have been compared in terms of predicted and actual widths of the regions of imperfect control, that is, in terms of $|\gamma|$. The comparison is not complete until it is illustrated that this predicted bound on $|\gamma|$ can be used to find a realistic state bound that compares to that which actually occurs. The technique of Chapter 5 applied to Case c for $|\gamma| = 1$, gives the (x_1,x_2) bound plotted in Figure 4.12. Superimposed on this is the (x_1,x_2) projection of the actual limit cycle that occurred. The result is found to be quite realistic.

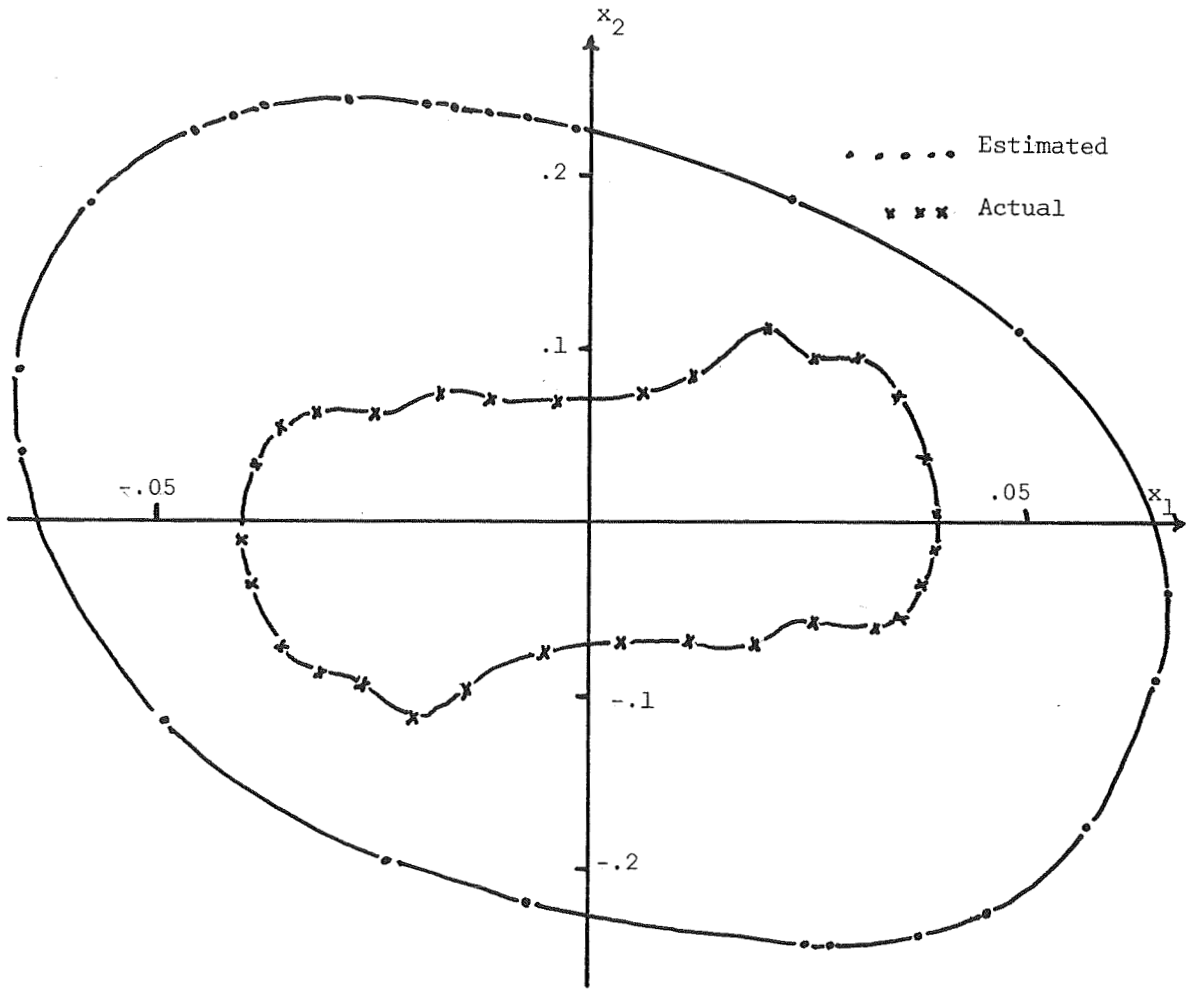

Comparison of Actual and Estimated Bounds for Case C

Figure 4.12

V. Determination of Bound on State Vector

The designs of Chapters III and IV were carried through to the determination of an invariant region of imperfect control. For the case of the augmented system design, this was a subset of the region of imperfect control which is the shaded part of Figure 3.7. In Chapter IV the characteristic of the natural switching function design guaranteed that the entire region of imperfect control was invariant. In this chapter the previous designs will be completed by calculating a state bound that results due to eventual confinement of the state vector to the region of imperfect control Ω.

Reduced-order System

It will now be shown that by nature of the fact that $\underline{x}$ will eventually be confined to the region of imperfect control

$$\Omega = \{\underline{x}: |\gamma(\underline{x})| \leq D\} \tag{5.1}$$

a reasonable bound can be determined for $\underline{x}$ by representing motion confined to Ω by a reduced-order system. The fact that $\underline{x} \in \Omega$ implies.

$$-D \leq \sum_{i=1}^{n} \alpha_i x_i \leq D. \tag{5.2}$$

Following through with the earlier assumption that $\alpha_n = 1$, the constraint implies

$$-D - \sum_{i=1}^{n-1} \alpha_i x_i \leq x_n \leq D \quad -\sum_{i=1}^{n-1} \alpha_i x_i \tag{5.3}$$

which is satisfied if

$$x_n = -\sum_{i=1}^{n-1} \alpha_i x_i + m(t) \tag{5.4}$$

where

$$|m(t)| \leq D. \tag{5.5}$$

In light of (5.5) it is possible to represent motion of (3.1) or (4.1) confined to Ω by the $(n-1)^{st}$-order system

$$\dot{\underline{x}}_r = A_r \underline{x}_r + \underline{c}_r m(t) \tag{5.6}$$

where A_r is an (n-1) x (n-1) matrix of the form

$$A_r = \begin{vmatrix} 0 & 1 & & \\ & 0 & 1 & \\ & & \ddots & \ddots \\ -a_1 & \cdots & & -a_{n-1} \end{vmatrix} \quad , \tag{5.7}$$

and $\underline{c}_r$ is an (n-1) x 1 vector of the form

$$\underline{c}_r = [0 \; \cdots \; 1]^T. \tag{5.8}$$

The reduced-order system (5.6) serves as a model that represents motion confined to Ω in that any solution of the latter is a solution of the former. Therefore, a bound on solutions of (5.6) is a bound on solutions of (3.1) or (4.1) confined to Ω. This represents another application of theorem (2.1).

It is important to note in (5.6) that the case $m \equiv 0$ represents motion confined to the switching hyperplane $\gamma=0$, and as pointed out earlier, the natural switching function design guarantees that this motion is asymptotically stable. Thus A_r is a stability matrix. Calculation of the bound on $\underline{x}$ confined to Ω is now accomplished by determination of the reachable set [10] of the linear time invariant stable reduced-order system. The term reachable set in this thesis denotes the set of points in (n-1) space that can be reached by trajectories of (5.6) starting at the origin and responding to the control m(t) which satisfies the convex constraint (5.5). No time limit is implied by this definition. To relate this to standard definitions this is the infinite time reachable set.

Reachable Set Calculation - Second-order Example

A computer estimation technique is available [9] whereby a piecewise-planar figure which bounds the reachable set, every facet of which touches the reachable set at one point, is obtained. A different method has been developed in this thesis. This method involves a computer simulation of (5.6) in which the impulse response is computed once during which time any number of points on the reachable set can be calculated. This scheme saves on computation time relative to the former method which requires a two-point-boundary-value problem solution for each facet of the approximation.

The method will first be illustrated for the second-order case. Extension is then made to the general case for which a digital computer program is outlined.

Consider the second-order system

$$\dot{\underline{x}} = A\,\underline{x} + \underline{c}\,m(t) \tag{5.9}$$

where

$$A = \begin{vmatrix} 0 & 1 \\ -1 & -1 \end{vmatrix}, \quad \underline{c} = \begin{vmatrix} 0 \\ 1 \end{vmatrix} \quad \text{and} \quad |m| \leq 1.$$

The problem is to find the boundary of this system's reachable set. Several important properties are known about the set [10]. It is bounded since A is a stability matrix, it is convex since the input constraint is convex, it includes the origin and it is symmetric with respect to the origin.

The reachable set of (5.9) is sketched in Figure 5.1. Convexity of this set implies that each point on the boundary such as the point p, must be an extremum of some variable such as y. That is to say, of all points on the boundary of the reachable set, p has the largest y component.

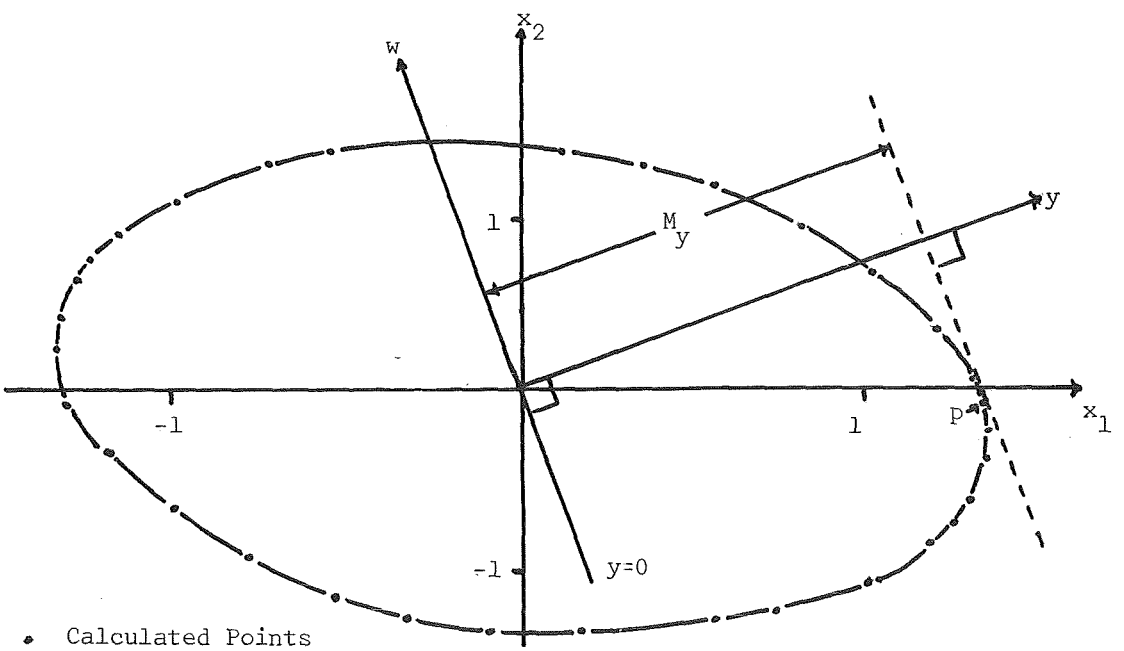

Figure 5.1
Reachable Set of (5.9)

The value of this largest y component M_y can be calculated by means of (2.58) to be

$$M_y = \int_0^\infty |h_y(\tau)| d\tau. \tag{5.10}$$

Here $h_y(t)$ is the inverse Laplace transform of $H_y(s)$, the filter

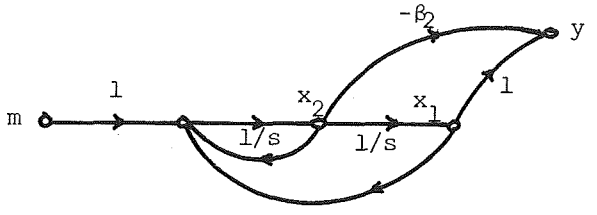

Figure 5.2

The Filter that Generates y

which relates the nodes m and y in Figure 5.2. Assuming

$$y = x_1 - \beta_2 x_2 \tag{5.11}$$

it results that

$$H_y(s) = \frac{Y(s)}{M(s)} = \frac{1-\beta_2 s}{s^2 + s + 1} \tag{5.12}$$

Although the computation of (5.10) involves an infinite-time integration an arbitrarily-close approximation may be obtained in finite time since $H_y(s)$ is stable.

It should be pointed out that this method only gives the y component of p. There is no direct method known for the calculation of the corresponding w component. However it will now be shown that this component can be calculated with the aid of another variable z the axis of which is closely aligned with that of y.

As shown in Figure 5.3 the point q of extreme z occurs close to p. The z component of q is given by

$$M_z = \int_{\infty} |h_z(\tau)| d\tau \qquad (5.13)$$

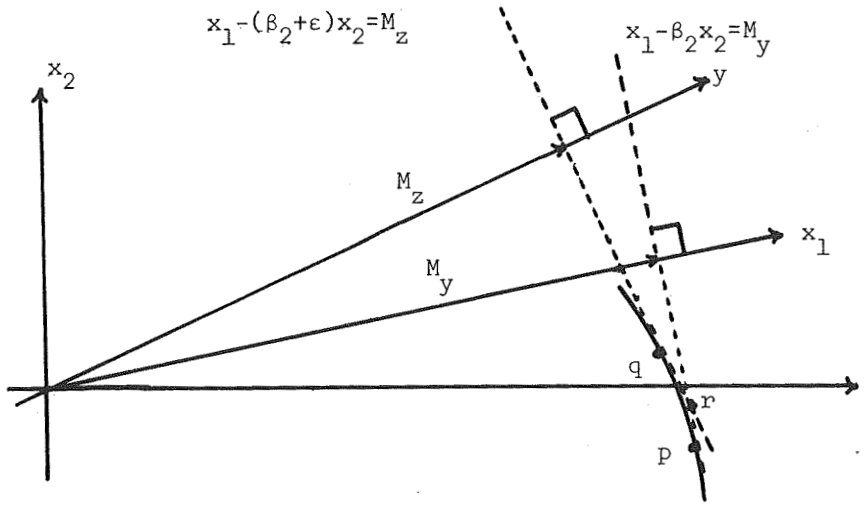

Figure 5.3

Calculation of a Point p on Reachable Set

where

$$z = x_1 - (\beta_2 + \epsilon)\, x_2 \qquad (5.14)$$

and correspondingly $h_z(t)$ is the inverse Laplace transform of

$$H_z(s) = \frac{1-(\beta_2 + \epsilon)\, s}{s^2 + s + 1} \qquad (5.15)$$

With the aid of the lines

$$x_1 - \beta_2 x_2 = M_y \qquad (5.16)$$

and

$$x_1 - (\beta_2 + \varepsilon)\, x_2 = M_z \tag{5.17}$$

which pass through the points p and q respectively and are parallel to the lines y = 0 and z = 0 respectively, both cooridnates of p will be calculated.

The intersection of (5.16) and (5.17) occurs at the point r which has coordinates

$$\begin{aligned} x_{1_r} &= (1 + \beta/\varepsilon)\, M_y - \frac{\beta}{\varepsilon} M_z \\ x_{2_r} &= \frac{1}{\varepsilon}\,[M_y - M_z]. \end{aligned} \tag{5.18}$$

In the limit as $\varepsilon \to 0$ it must be that $p \to q$ and therefore $r \to p$. The coordinates of p are

$$\begin{aligned} x_{1_p} &= \lim_{\varepsilon \to 0} x_{1_r} \\ x_{2_p} &= \lim_{\varepsilon \to 0} x_{2_r}. \end{aligned} \tag{5.19}$$

In the computer calculation of these coordinates, ε is chosen to be small in comparison to β_2. Extremely small values are not used due to computer round-off error being significant. The numbers M_y and M_z are calculated by starting the system (5.9) at the initial condition $x_1 = 0$, $x_2 = 1$ and setting $m(t) \equiv 0$. This is equivalent to applying an impulse at m(t). The signals y(t) and z(t), generated according to (5.11) and (5.14), are then the impulse responses $h_y(t)$ and $h_z(t)$ respectively. Their absolute integrals are calculated to give M_y and M_z according to (5.10) and (5.13) with the upper time limit set to be large in comparison with the largest time constants of the filters $H_y(s)$ and $H_z(s)$. In this manner the point p is calculated by solving the system dynamics only once. The same is true of the following method of calculating any number of points on the reachable set boundary.

The variables y and z are defined in terms of β_2. By varying β_2 over a number of discrete values between $-\infty$ and $+\infty$ the same number of variables y_i and z_i will be defined. The system dynamics are then solved once to give M_{y_i} and M_{z_i} for all i. For each set of these

values a point on the boundary is calculated. Each point is reflected through the origin to complete the picture. For the system of (5.9) this technique gave the points indicated in Figure 5.1.

Reachable Set - General Case

The preceding discussion will now be generalized to obtain a point on the boundary of the reachable set of the $(n-1)^{st}$-order system (5.6). Define y to be now

$$y = \beta^T \underline{x}_r = \sum_{i=1}^{n-1} \beta_i x_i \tag{5.20}$$

where we assume $\beta_1 = 1$. It is now necessary to define (n-2) axes whose direction are close to that of y. They are denoted by

$$z_j = y + \varepsilon_j x_j; \quad j=2,3,\ldots(n-1). \tag{5.21}$$

The variable y(t) and the (n-2) variables $z_j(t)$ are generated from the (n-1) states x_i as they respond to the initital condition $x_1 = x_2 = \ldots = x_{n-2} = 0$, $x_{n-1} = D$ in accordance with (5.6) with $m(t) \equiv 0$. Once again, this is equivalent to applying an impulse input m(t) with area D. The absolute values are integrated for a sufficient long time to give

$$M_y = \int_0^\infty |y(\tau)| d\tau \tag{5.22}$$

and

$$M_{z_j} = \int_0^\infty |z_j(\tau)| d\tau \qquad j=2,3,\ldots(n-1). \tag{5.23}$$

The resulting point on the reachable set is then the solution of the following set of (n-1) equations in the (n-1) unknowns

$$\sum_{i=1}^{n-1} \beta_i x_i = M_y \tag{5.24}$$

$$\sum_{i=1}^{n-1} \beta_i x_i + \varepsilon_j x_j = M_{z_j}; \quad j=2,3,\ldots(n-1).$$

This can be achieved by solving (5.6) only once. This is again true

also of the case wherein any number of points on the reachable set boundary are to be calculated. In this case, a set of variables is defined for each set of values of each β_i and the calculations corresponding to (5.22), (5.23) and (5.24) could all be made simultaneously.

This completes the treatment of reachable set calculations that are used in this thesis to evaluate state bounds that result due to motion of the state vector confined to the regions of imperfect control derived in Chapters III and IV.

VI. CONCLUSIONS

A new design was proposed for model-reference controllers. In contrast to others, it led to a controlled system in which the affects of several forms of imperfection could be evaluated. It was shown that the choice of a linear model that had at least one real eigenvalue, facilitated the use of what was termed a natural switching function. Such a switching function was shown to guarantee that the error state vector would monotonically approach the switching plane until it entered a certain planar neighborhood of the switching plane, termed the region of imperfect control. Upon entering this region, the state vector was forced by the natural switching function design to remain in the region for all subsequent time. It was this property that enabled the state bound to be calculated.

The results concerning model-reference controllers were developed in Chapter IV. At the onset, one very important conclusion was conveniently made by use of the Kalman-Meyer lemma represented in 2.14. That is that asymptotic stability of a phase-variable model-reference controller cannot be guaranteed for the case wherein the highest-order state does not appear in the switching function. A considerable effort was spent investigating the converse before the lemma appeared in the literature. The problem stemmed from the very cumbersome Liapunov equation (2.4). This result led to the need for developing a Lagrange type bound.

The relevance of the natural switching function design cannot be overemphasized. It was this design which facilitated the subsequent bound development.

Two intuitive results concerning the bound are proved in Chapter IV. The first is that in the case of a system with a far-out pole, the highest-order state may be eliminated from the control law with very small resultant error bound. The second is that in the absence of measurement noise, the highest-order state may be replaced with the derivative of the next-highest-order state with very small resultant error bound.

By far the most important result of Chapter IV was represented by the simulation data from the example. The data tabulated in Figure 4.9 was based solely on the relay control system model (4.38) and (4.39)

of the model-reference control system (4.32). The conservativeness of the results was therefore affected by the degree to which the parameter $b_3(t)$ in actuality approached the worst case. Figures 4.10 and 4.11 demonstrated that the bounds predicted by Figure 4.9 were realistic. These results demonstrated the relevance of the modelling theorem (2.1).

One question left unanswered by the development of Chapter V pertained to the degree to which the reachable set bound compared to an actual bound that would occur. The result in Figure 4.12 showed that this could be quite realistic.

The primary result of Chapter V was the development which led to the numerical technique generalized at the end of the chapter. This provides an area for future research. The geometrical approach to the reachable set calculation shows some promise of leading to new results concerning properties of these sets and possibly closed-form expressions of their boundaries.

The results of Chapter III, though tangential to the main object of the thesis, are considered to be of theoretical importance. This material involved a new concept; that of allowing the Liapunov function to decrease in a non-monotone fashion. This idea is interesting in that it offers a practical alternative to asymptotic stability. The design example illustrated the utility of the concept and suggests two areas for future research. The fact that the actual Liapunov function of the original system was monotonic nonincreasing implies that perhaps this could be guaranteed analytically. Secondly, there is a need to simplify the associated algebra required to guarantee positive realness of the augmented transfer function G'(S).

Bibliography

1. Grayson, L. P., "Design via Liapunov's Second Method," Preprints of Technical Papers, Fourth JACC, Prepared by A. I. Ch. E., New York, N. Y., 1963, pp 589-595.

2. Monopoli, R. V., "Engineering Aspects of Control System Design Via the 'Direct Method' of Liapunov". N.A.S.A. Report C. R. 654, October, 1966, Office of Technical Services, Department of Commerce, Washington, D. C., 20230.

3. Lindorff, D. P., "Control of Nonlinear Multivariable Systems", I.E.E.E. Transactions, AC-12, #5, October, 1967.

4. Taylor, T. M., Determination of a Realistic Error Bound for a Class of Imperfect Controllers, JACC Preprints, Ann Arbor, Mich., 522-538 (1968).

5. Hahn, W., "Theory and Application of Liapunov's Direct Method" (in German) English Translation, Prentic-Hall, Inc., Englewood Cliffs, N. J., 1963.

6. Kalman, R. E., "Liapunov Functions for the Problem of Lure in Automatic Control," Proc. Nat'l Acad. Sci., Vol. 49, pp 201-205, February, 1963 (Main Lemma).

7. Meyer, K. R., "Liapunov Functions for the Problem of Lure", Proc. National Academy of Science, Vol. 53, pp. 501-503, 1965.

8. LaSalle, J. P., "Some Extensions of Liapunov's Second Method", I.R.E. Transactions on Circuit Theory, CT-7 (1960), 520-527.

9. Pecsvaradi, T., and Narendra, K. S., Reachable Sets for Linear Dynamical Systems, Dunham Laboratory Technical Report CT-29, July 1969, Department of Engineering and Applied Science, Yale University.

10. LeMay, J. L., "Recoverable and Reachable Zones for Control Systems with Linear Plants and Bounded Controller Outputs," Preprints, JACC, Stanford, California, June, 1964, pp. 305-311.

11. Gantmacher, F. R., The Theory of Matrices, Vol. 2, Chelsea Publishing Co., New York, N. Y.(1964).

12. Goldstein, B. F., and Lindorff, D. P., "A Stability Bound for Relay Control Systems in Non-Phase Variable Form", Proceedings Third Asilomar Conference on Circuit and System Theory, December, 1969.

13. Bass, R. W., discussion of a paper by A.M. Letov, Proc. Heidelberg Conf. on Automatic Control ("Regelungs Technik: Moderne Theolien and ihre Verwendbarkedt," by R. Oldenbourg, Munich, 1957),pp 209-210.

NATIONAL AERONAUTICS AND SPACE ADMINISTRATION
WASHINGTON, D.C. 20546

OFFICIAL BUSINESS

FIRST CLASS MAIL

POSTAGE AND FEES PAID
NATIONAL AERONAUTICS AND
SPACE ADMINISTRATION

POSTMASTER: If Undeliverable (Section 158 Postal Manual) Do Not Return

"The aeronautical and space activities of the United States shall be conducted so as to contribute . . . to the expansion of human knowledge of phenomena in the atmosphere and space. The Administration shall provide for the widest practicable and appropriate dissemination of information concerning its activities and the results thereof."

—NATIONAL AERONAUTICS AND SPACE ACT OF 1958

NASA SCIENTIFIC AND TECHNICAL PUBLICATIONS

TECHNICAL REPORTS: Scientific and technical information considered important, complete, and a lasting contribution to existing knowledge.

TECHNICAL NOTES: Information less broad in scope but nevertheless of importance as a contribution to existing knowledge.

TECHNICAL MEMORANDUMS: Information receiving limited distribution because of preliminary data, security classification, or other reasons.

CONTRACTOR REPORTS: Scientific and technical information generated under a NASA contract or grant and considered an important contribution to existing knowledge.

TECHNICAL TRANSLATIONS: Information published in a foreign language considered to merit NASA distribution in English.

SPECIAL PUBLICATIONS: Information derived from or of value to NASA activities. Publications include conference proceedings, monographs, data compilations, handbooks, sourcebooks, and special bibliographies.

TECHNOLOGY UTILIZATION PUBLICATIONS: Information on technology used by NASA that may be of particular interest in commercial and other non-aerospace applications. Publications include Tech Briefs, Technology Utilization Reports and Notes, and Technology Surveys.

Details on the availability of these publications may be obtained from:

SCIENTIFIC AND TECHNICAL INFORMATION DIVISION

NATIONAL AERONAUTICS AND SPACE ADMINISTRATION

Washington, D.C. 20546